MODELING AND OPTIMIZATION ON ENERGY COSTS IN INTERNAL THERMALLY COUPLED DISTILLATION COLUMNS OF NON-IDEAL MIXTURES

Xinggao Liu* **and** **Jixin Qian**

Institute of Systems Engineering, Department of Control Science and Engineering,
Zhejiang University, Hangzhou 310027, PR China,
Email address: liuxg@iipc.zju.edu.cn

Abstract: Internal Thermally Coupled Distillation Column (ITCDIC) is the frontier of energy saving distillation research. In this paper, an evaluation method on the operating cost and its saving in the ITCDIC processes of non-ideal mixtures is presented. A mathematical model for optimization is first derived. The ethanol-water system is studied as an illustrative example. The optimization results show that the ITCDIC process of non-ideal mixture possesses an enormous potential of operating cost saving. The optimal operation conditions and the maximum percentage of operating cost saving are obtained simultaneously. The process analysis is then carried out and the results show the necessity and importance of optimal design on the rectifying pressure, the feed thermal condition, and the total heat transfer rate. These pave the way for the smooth operation and the further optimal design of ITCDIC processes for non-ideal mixtures.

Keywords: distillation columns, modeling, optimization, process analysis.

1. INTRODUCTION

Distillation remains the most important method used in the chemical industry for the separation of homogeneous mixtures with the amount of energy used in distillation operations being considerable. It takes heat from a heat source at bottom and generally reject most of this heat to a heat sink at the top while performing the task of separation for a conventional distillation column (CDIC), and is thus well known that the CDIC is both energy intensive and inefficient. If the energy removed from the rectifying section could be reused in the stripping section or waste heat was available, energy savings would be achieved in a distillation column.

Energy recovery by heat transfer from the rectifying section to the stripping section is an effective method for energy savings in distillation columns. This method, first proposed by Mah et al. (1977), is called the SRV method. An ITCDIC is constructed in such a manner that the rectifying section and the stripping section are separated into two columns, a compressor and a throttling valve are installed between the two sections and the internal thermal coupling is accomplished through a heat exchanger between them as shown in Fig.1 (Liu, and Qian, 2000), where energy saving is realized by the SRV method, which however has neither a reboiler nor a condenser, can be operated smoothly with two decentralized PID controllers and offers some distinct advantages over CDIC (Liu and Qian, 2000, Huang et al., 1997; Huang et al., 1999).

*To whom correspondence should be addressed.

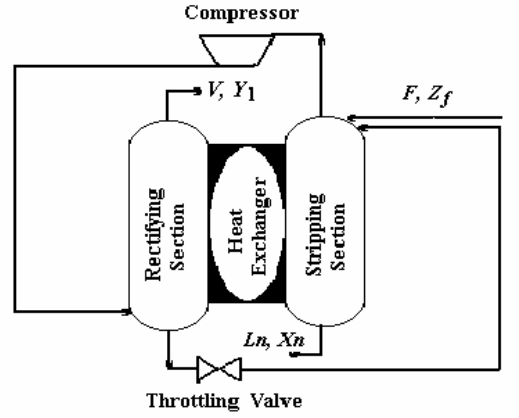

Fig. 1. Schematic diagram of ITCDIC

Because of the internal thermal coupling, a certain amount of heat is transferred from the rectifying section to the stripping section and brings the downward reflux flow for the former and the upward vapor flow for the latter. As a result, the condenser and the reboiler are not required and energy savings are realized. The research of Liu and Qian (2000) has shown that the energy saving could be up to 40-50% compared with CDIC. However, considering the compressor in an ITCDIC uses electric energy, which often takes two or three times more heat energy to generate a unit quantity of work energy and is generally much more expensive than the low-level steam needed by a CDIC, it is very important to explore the operating cost and its saving potential, which is one of the key to decide if the ITCDIC could be widely used. The approach is confirmed by the fact that energy costs usually far exceed the investment costs of a distillation column (Doukas and Luyben, 1978). But how about the operating cost of an ITCDIC, is it economic compared with a CDIC? How much on earth could the operating cost saves? How much is the operating cost saving potential of an ITCDIC process? Little, however, has appeared in the literature on these matters.

The aim of the present work is to explore the operating cost in an ITCDIC of a non-ideal mixture. An evaluating method on energy cost is proposed and a mathematical model for optimization on the energy cost saving potential in an ITCDIC process is then derived. The optimal assessments on the operating cost saving and the related process analysis are carried out, which pave the way for further optimal design of ITCDIC for non-ideal mixtures. From our knowledge, up to now, no one has worked on this matter.

2. EVALUATION OF OPERATING COST

A steady state ITCDIC process of a non-ideal mixture is considered. A CDIC under the minimum reflux ratio operating is chosen as a basis for comparison and assessment of the ITCDIC.

The operating cost of an ITCDIC process includes the cost of electric energy consumed by the compressor, the stream cost to preheat feed and the cooling water cost to cool the vapor distillate. It can be calculated as,

$$C_{ITCDIC} = W_{comp}\, UP_{electric} + Q_{preheat,ITCDIC}\, UP_{steam} + Q_{cool,ITCDIC}\, UP_{cool} \quad (1)$$

where W_{comp} is the load of the compressor. The adiabatic compression and the compression efficiency, η, are considered, therefore W_{comp} can be calculated as

$$W_{comp} = V_f\, k / (k\text{-}1) RT_{in}((P_{out} / P_{in})^{(k-1)/k} \text{-}1) / \eta \quad (2)$$

The loads of both preheating feed and cooling the vapor distillate are respectively calculated as,

$$Q_{preheat,\,ITCDIC} = F(1\text{-}q)\Delta H_{F,v} \quad (3)$$

$$Q_{cool,ITCDIC} = V_1\, \Delta H_{cool,\,v} \quad (4)$$

The operating cost of a CDIC process operated at the minimum reflux ratio, which is also the minimum operating cost of the CDIC process, is chosen as the comparison basis of the ITCDIC operating. The percent operating cost saving of the ITCDIC process is defined as,

$$X_C = (C_{rmin,CDIC} - C_{ITCDIC}) / C_{rmin,CDIC} \quad (5)$$

where $C_{rmin,CDIC}$ is the operating cost of the CDIC process operated at the minimum reflux ratio, which includes the steam cost for both preheating feed and consumed by the reboiler, and the cooling water cost of the condenser in the CDIC process.

3. A MATHEMATICAL MODEL FOR OPTIMIZATION

The optimization model of the ITCDIC for a non-ideal mixture is derived by applying energy, component and overall material balances, and vapor-liquid equilibrium under the following assumptions:
(1) Perfect liquid and vapor mixing on each tray, the temperature and the composition on each tray being uniform; (2) Vapor-liquid equilibrium for streams leaving each tray; (3) Instantaneous heat transfer from the rectifying section to the stripping section and the transportation of liquid and vapor between trays; (4) Negligible pressure drop and heat loss in each column.

3.1 Objective function

In order to explore the operating cost in the ITCDIC process of a non-ideal mixture, the percent energy cost saving of the ITCDIC, X_C, is chosen as the objective function, which shows the energy cost saving effect directly and could be calculated from Eq. (5) together with Eqs. (1)-(4).

The design parameters including the pressure of the rectifying section, *Pr*, the feed thermal condition, *q*, and the total heat transfer rate, *UA*, are chosen as the optimized parameters. The optimization goal is to find the optimal values of *Pr*, *q*, and, *UA* and obtain the maximums of the operating cost saving of the ITCDIC compared with those of CDIC operated at the minimum reflux ratio, while the product qualities are guaranteed simultaneously.

3.2 Equality constraints

The stages are numbered with the top as Stage 1 and the bottom as Stage n. The amount of thermal coupling in the ITCDIC is then calculated from the following equation (Mah et al., 1977),

$$Q_j = UA(T_j - T_{j+f-1}) \quad j=1,\ldots,f-1 \tag{6}$$

The stage temperature can be calculated by Antoine Eq. (7) and the vapor saturation pressure of the *i*th component at the *j*th stage is calculated by Eq. (8)

$$T_j = b/(a - LnP_{vp,ij}) - c \tag{7}$$

$$P_{vp,ij} = P\, Y_{ij} / (\gamma_{ij} X_{ij}) \tag{8}$$

where γ_{ij} is the activity coefficient for the *i*th component at the *j*th stage.

From the component material balance, the following equations are derived,

$$V_2 Y_{i2} - V_1 Y_{i1} - L_1 X_{i1} = 0 \quad j=1 \tag{9}$$

$$V_{j+1} Y_{i,j+1} - V_j Y_{i,j} + L_{j-1} X_{i,j-1} - L_j X_{i,j} = 0 \quad j=2,\ldots,n-1 \text{ and } j \neq f \tag{10}$$

$$V_{f+1} Y_{i,f+1} - V_f Y_{i,f} + L_{f-1} X_{i,f-1} - L_f X_{i,f} + FZ_{iF} = 0 \quad j=f \tag{11}$$

$$- V_n Y_{i,n} + L_{n-1} X_{i,n-1} - L_n X_{i,n} = 0 \quad j=n \tag{12}$$

According to the total mass balances, the liquid and vapor flow rates are derived as follows

$$L_j = \sum_{k=1}^{j} Q_k / \lambda \quad j=1,\ldots,f-1 \tag{13}$$

$$L_{f+j-1} = L_{f-1} + Fq - \sum_{k=1}^{j} Q_k / \lambda \quad j=1,\ldots,f-2 \tag{14}$$

$$Ln = F - V_1 \tag{15}$$

$$V_1 = F(1-q) \tag{16}$$

$$V_{j+1} = V_1 + L_j \quad j=1,\ldots,f-1 \tag{17}$$

$$V_{f+j} = V_f - F(1-q) - \sum_{k=1}^{j} Q_k / \lambda \quad j=1,\ldots,f-2 \tag{18}$$

From the Vapor-Liquid equilibrium relationships, the vapor composition is obtained as

$$Y_{ij} = K_{ij} X_{ij} \tag{19}$$

where K_{ij} is the equilibrium vaporization ratio and can be calculated from Eq. (20). For a lower pressure system (generally, less than 1.013MPa), it can be simplified as Eq. (20a).

$$K_{ij} = (\gamma_{ij} f^{0}_{ij}) / (\varphi^{V}_{ij} P) \tag{20}$$

$$K_{ij} = \gamma_{ij} P_{vp,ij} / P \tag{20a}$$

where f^{0}_{ij} is the liquid fugacity for the *i*th component at the *j*th stage under a standard state, φ^{V}_{ij} is the gas fugacity coefficient for the *i*th component at the *j*th stage.

Eqs. (6)-(20) constitute the equality constraints of the optimization model of an ITCDIC.

3.3 Inequality constraints

For different product qualities, such as top product composition $Y_1 \geq 80\%$ (mole fraction), bottom product composition $X_n \leq 25\%$ or $Y_1 \geq 75\%$, $Xn \leq 20\%$, they have different optimal values of the design parameters. Constraints should be thereby set on product qualities. For Example, for the controlled compositions

$$Y_{i1} \geq Y_{i,\text{setpoint}}, \quad X_{in} \leq X_{i,\text{setpoint}} \quad etc. \tag{21}$$

For the total separation effect, there is

$$FZ_{iF} \geq V_1 Y_{i1} \tag{22}$$

The proper region of the optimized variables must be specified, such as

$$Pr \in [0.1013, 1.013] \text{ Mpa} \tag{23}$$

$$q \in [0, 1] \tag{24}$$

$$UA \in [7500, 15000] \text{ W}\cdot\text{K}^{-1} \tag{25}$$

In order to prove the practicality and feasibility of the composition solution, the following constraints should be set

$$X_{ij} \in [0, 1] \tag{26}$$

$$Y_{ij} \in [0, 1] \tag{27}$$

Eqs. (21)-(27) constitute the inequality constraints of the optimization model of an ITCDIC. Therefore the optimization task can be written as follows

ITCDIC Minimize $f(Pr, q, UA) = -X_c$ (ECSOPT)

Subject to the equality constrains, Eqs. (6-20)

and to the inequality constrains, Eqs. (21-27)

It is a nonlinear programming (NP) constrained optimization problem. A reduced Eq.-oriented Solution Technique1 (Piela et al., 1991), is used to solve process flow-sheet. The Successive Quadratic Programming (SQP) method (Schmid and Biegler, 1994), is used as the optimization algorithm.

4. OPTIMIZATION AND ANALYSIS

In following optimization, a 68-stage ITCDIC is

considered as an illustrative example, where a non-ideal mixture of ethanol-water is separated. The maximum of the operating cost saving of the ITCDIC is explored with the maximum of the percent operating cost saving of ITCDIC as the optimal objective function. The energy prices are shown in Table 11 (Ferre et al., 1985). The compressor is assumed to operate with a mechanical efficiency of 80% and be driven by electric motors. The use of a 90% on-stream factor is also assumed. Wilson's method is adopted in the vapor-liquid equilibrium calculation. The operating conditions are listed as follows:

Total number of stages	68
Feed stage	35
Feed flow rate	0.1 kmol·s^{-1}
Feed composition, ethanol/water	0.5/0.5
Top product quality (ethanol)	≥ 80%
Bottom product quality (ethanol)	≤ 25%
Pressure of stripping section	0.1013Mpa

Table 1 Cost of utilities

Utility	Price
Steam	0.0095 $/kg
Cooling water	0.05 $/m^3
Electrical energy	0.06 $/kW·hr

Table 2 lists the optimization results of the ethanol-water system, when top product composition Y_1 ≥80% (mole fraction), bottom product composition, X_n ≤25%. The detailed optimized regions of the optimized variables are given in the table.

The optimization result shows that the maximum of the percent energy cost saving for ethanol-water separation in the ITCDIC process is 38.26% compared with the operating cost of the CDIC operated the minimum reflux ratio, which is absolutely striking and attractive. It reveals that the ITCDIC process of non-ideal mixture possesses a high industrial application value and an enormous economical prospect.

Table 2 The maximum operating cost saving of ITCDIC for the ethanol-water system

		Optimized regions	Optimal results
Quality target	Y_1, %	≥80	80.11
	X_n, %	≤25	25
Optimized variables	*Pr*, MPa	0.1013~1.013	0.1334
	q	0~1	0.5463
	UA, W.K^{-1}	7500~15000	15000
Goal	Maximum operating cost saving, X_C , %		38.26

Table 3 lists the detailed energy loads and the related operating costs for ethanol-water separation in the ITCDIC process under the optimal operation condition listed in Table 2 and those of the CDIC operated at the minimum reflux ratio. The results show although an infinite number of stages are necessary for the theoretical minimum reflux condition (minimum energy requirement) in a CDIC process, the ITCDIC of a non-ideal mixture can operate with energy cost requirements much more less than that of the minimum value for a CDIC. In the studied case, the operating cost saving for ITCDIC compared with the minimum operating cost of CDIC is 0.214 million dollars annually, which reveals the enormous economical prospect in the ITCDIC process of the non-ideal mixture.

Table 3 Energy loads and operating costs for the ethanol-water system

	CDIC		ITCDIC	
	Load, kW	Cost, K$/Y	Load, kW	Cost, K$/Y
Reboiler	1579	217.33	——	——
Preheating feed	1799	247.66	1799	247.66
Cooling	3334	95.40	1778	50.74
Compressor	——	——	84.33	47.57
Total		560.39		345.97

The optimal results in Table 2 and the operating load and cost results in Table 3 reveal that the ITCDIC process for non-ideal mixture can save more energy cost. Based on the optimization program and the optimal results, the following discussion and process analyses are explored and some useful conclusions are obtained as follows:

(1) From the optimal result and the optimal region of the pressure in Table 2, it is seen that the optimal operating pressure of the rectifying section is about 1.5 atmospheric pressures, which is easy to be realized. Fig 2 shows that while the operating pressure of the rectifying section is higher than the optimal operating value, the energy cost saving effect decreases with the operating pressure, which could be explained by the following theoretical analysis. Theoretically, the pressure difference between the rectifying and stripping sections provides the necessary operating driving force for the ITCDIC, with the increasing of the operating pressure of the rectifying section, the operating driving force hereby is increasing, which profit the separation effect. However, the work of the compressor is increasing accordingly and the percent energy cost saving of the ITCDIC is thus then decreasing.

From the curve of *Pr*- X_c in Fig. 2, it can be seen that

the pressure of the rectifying section, *Pr*, has a great effect on the percent operating cost saving in an ITCDIC process and they have a obvious non-linearity. It reveals that optimal design on *Pr* is very important to realize an economical ITCDIC operation of non-ideal mixture.

(2) Table 4 shows the effect of the feed thermal condition, *q*, on X_c and production quality while the other conditions of the optimal results in Table 2 are kept constant. While *q* is increasing, Y_1 is increasing, but the bottom composition cannot satisfy the quality constraints; while *q* is decreasing, X_c is decreasing and the top composition cannot satisfy the quality constraints, but the bottom composition is purer.

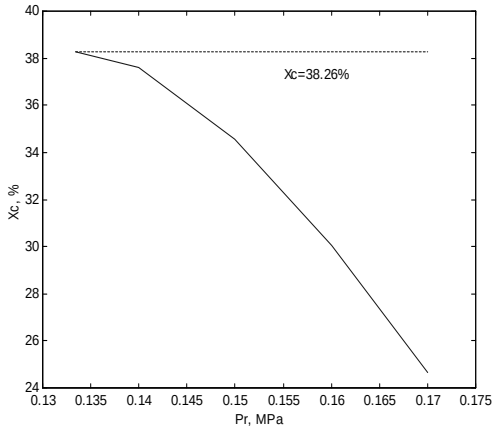

Fig. 2. The changes of the percent energy cost saving of ethanol-water mixture in the ITCDIC process, when P_r changes from 0.1334 to 0.5065 MPa and the other operation conditions of the optimal results in Table 2 are kept constant.

Table 4 Effect of the feed thermal condition on X_c and production quality for the ethanol-water mixture, while the other conditions of the optimal results in Table 2 are kept constant

	Optimal value	When q is changed from the optimal results of Table 2					
	q=0.5463	3%	6%	9%	-3%	-6%	-9%
Y_1, %	80.11	80.45	80.78	81.11	79.74	79.36	78.95
X_n, %	25	26.33	27.62	28.87	23.62	22.19	20.72
X_c, %	38.26	38.63	38.97	39.28	37.87	37.44	36.98

These reveal the complexity among *q*, X_c and the quality targets, which implies that the optimization procedure on *q* is necessary to gain the proper optimal design value of *q* in an ITCDIC process of a non-ideal mixture. From the change scale of Y_1, X_n and X_c in Table 4 while *q* changes, it shows that the feed thermal condition, *q*, has a great effect on Y_1, X_n and X_c and the optimal design on the feed thermal condition, *q*, is very important for the proper ITCDIC operation.

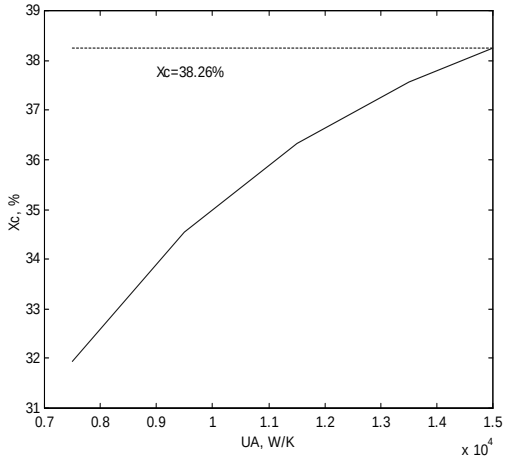

Fig. 3. The changes of percent operating cost saving for ethanol-water system, when *UA* changes from 7500 to 15000 W/K and the other operation conditions of the optimal results in Table 2 are kept constant.

(3) Table 2 shows that the optimal value of the heat transfer rate for the ethanol-water mixture is the upper boundary under the goal of the maximum of the energy cost saving. This implies that for the ethanol-water system, the increase of the heat transfer rate is beneficial for the energy saving of the ITCDIC process as shown in Fig. 3, which shows the influence of *UA* on the percent operating cost saving for the ethanol-water system, while the other conditions of the results in Table 2 are kept constant. In the view of the theory, with the increasing of the heat transfer rate, the amount of the thermal coupling, calculated by equation (6), is increasing, which is profitable to the ITCDIC process and the energy cost is, hereby, reduced under the same finite separation effect.

Fig 3 also reveals that *UA* has a great and complicated effect on X_c. It is thus very important to design an optimal valve of *UA* for a proper ITCDIC operation.

5. CONCLUSIONS

In this work an evaluating procedure of energy cost in the ITCDIC process of a non-ideal mixture is proposed. A mathematical model for optimization on the operating cost saving potential is derived, which include the comparison with the energy consumption and the operating cost of the CDIC operated at the minimum reflux ratio. The optimization and process analysis of ethanol-water system are carried out.

Optimization results show that the ITCDIC of non-ideal mixture possesses a high potential of energy cost saving. Through the optimization of the energy cost saving, it is found that the maximum percent energy cost saving for non-ideal mixtures in the ITCDIC process is close to 40% compared with the

operating cost of the CDIC under the minimum reflux ratio operating. It reveals that the ITCDIC process of the non-ideal mixture possesses a high industrial application value and an enormous economical prospect.

Process analysis results show that there exists an optimal design problem for selecting the rectifying pressure, *Pr*, the feed thermal condition, *q*, and the total heat transfer rate, *UA*, in the ITCDIC process of the non-ideal mixture and there are very complicated relations among the energy cost parameters, the product qualities and the optimized variables. It is also found that the optimal operating pressure of the rectifying section is easy to be realized, and while the operating pressure of the rectifying section is higher than the optimal operating value, the energy cost saving effect decreases with the operating pressure. Bearing these in mind is very important for the smooth operation and the optimal design of an ITCDIC process for a non-ideal mixture.

Based on the study of this paper, we have developed a related optimization software 'ECSOPT', which is a convenient tool for quick calculation of the maximum energy cost saving potential and the optimum values of the design variables for the ITCDIC process of non-ideal mixture, and is thereby very useful and significant to further researches on ITCDIC processes of non-ideal mixtures.

ACKNOWLEDGEMENTS

This work is supported by National Natural Science Foundation of China (NSFC, No. 20106008), and its support is herein acknowledged.

NOMENCLATURES

F	feed rate, kmol·s^{-1}
k	adiabatic index number of gas
K	equilibrium vaporization ratio
L	liquid flow rate, kmol·s^{-1}
P	representation of either Pr or Ps, MPa
Pr	pressure of rectifying section, MPa
Ps	pressure of stripping section, MPa
P_{vp}	vapor saturation pressure, MPa
q	feed thermal condition
Q	energy demand, W
T	absolute temperature, K
UA	heat transfer rate, W·K^{-1}
UP	unit price of loads, \$·W^{-1}
V	vapor flow rate, kmol·s^{-1}
W	thermodynamic work, W
X	mole fraction of liquid
X_c	percent operating cost saving
Y	mole fraction of vapor
Z_F	mole fraction of feed
λ	latent heat of vaporization, kJ·kmol^{-1}
γ	activity coefficient

Subscripts

comp	compressor
f	feed stage
F	feed
i	component
j	stage number

REFERENCES

Doukas, N. and W.L. Luyben, (1978). Economics of alternative distillation configurations for the separation of ternary mixtures. *Ind. Eng. Chem. Process Des. Dev.*, **17**, 273.

Ferre, J.A., F. Castells and J. Flores (1985). Optimization of a distillation column with a direct vapor recompression heat pump. *Ind. Eng. Chem. Process Des. Dev.* **24(1),** 128−132.

Huang, K.J., J.X. Qian, D.Z. Zhan, et al (1997). Steady-state operation analysis of an ideal heat integrated distillation column. *Chinese J. Chem. Eng.*, **5(4),** 325−336.

Huang, K.J., D.Z. Zhan, et al (1999). Control of ideal heat integrated distillation columns. *Chinese J. Chem. Eng.*, **7(4),** 283-294.

Liu, X.G. and J.X. Qian (2000). Modeling, Control, and Optimization of Ideal Internal Thermally Coupled Distillation Columns. *Chem. Eng. Technol***., 23(3)**, 235-241.

Mah, R.S.H., J.J. Nicholas and R.B. Wodnik (1977). Distillation with secondary reflux and vaporization: a comparative evaluation. *AIChE J.*, **23(5),** 651−658.

Piela, P.C., T.G. Epperly, K.M. Westerberg and A.W. Westerberg (1991). ASCEND, an object-oriented environment for modeling and analysis: the modeling language. *Comp. Chem. Eng*., **15(1)**, 53−72.

Schmid, C. and L.T. Biegler (1994). Quadratic programming methods for reduced hessian SQP. *Comp. Chem. Eng.*, **18**, 817−832.

MULTI-OBJECTIVE ROBUST CONTROL OF AN EVAPORATION PROCESS

Wenjun Yan [*,1] **Yi Cao** [**]

[*] *Department of Systems Science and Systems Engineering, Zhejiang University, Hangzhou, 310027, China, email: yanwenjun@zju.edu.cn*

[**] *Department of Process and Systems Engineering, Cranfield University, Bedford, MK43 0AL, U.K., email: y.cao@cranfield.ac.uk*

Abstract: In this paper, a new multi-objective robust control design approach is applied to an evaporation process. The new approach, proposed in (Yan and Cao, 2002) extends the standard generalized-l_2 (Gl_2) control problem based on a new Lyaponov stability condition to a set of new linear matrix inequality (LMI) constraints such that the multi-objective robust control problem associated with robust stability and robust performance objectives can be less conservatively solved using computationally tractable algorithms. A comparison of simulation results with controllers designed by different techniques demonstrates the superiority of the new method.

Keywords: Generalized l_2 synthesis, Multi-objective optimization, Robust Controller, Discrete linear time-invariant system, Evaporation process

1. INTRODUCTION

In the last two decades, many analysis and synthesis approaches in control theory have been developed. Among those control strategies, multi-objective control and robust control have obtained more and more attractions. The former is to resolve the inherent trade-offs among conflictive design specifications. Many control strategies have been studied in this aspect, such as H_∞, H_2, mixed H_2/H_∞ and mixed L_1/H_∞. More details can be found in (Scherer *et al.*, 1997) and reference therein. Nominal systems are mainly considered with these methodologies.

On the other hand, due to uncertainty in practical systems, robustness of control systems has to be taken into account. In H_∞ design, disturbances and uncertainties are lumped into a single norm rather than bounded separately. This certainly leads to some conservatism. In contrast, the μ-synthesis technique overcomes the conservatism by introducing structured uncertainty blocks. However, the optimization has to be solved via a so-called D-K iteration, in which the joint convexity is not guaranteed although individual step(K-step or D-step) is convex. Hence, it may become computationally intractable (Skogestad and Postlethwaite, 1996) to achieve a globally optimal performance. As it was pointed out by Toker and Ozbay (1995), most robust synthesis problems proposed so far are NP-hard and computationally intractable. However, by combining the concepts of H_∞ optimization, linear matrix inequalities (LMI) and integral quadratic constraints, a convex solution to a large class of robust and optimal control problems, the generalized-l_2 (Gl_2) formulation has been proposed by D'Andrea (1999)

[1] Supported by the China Scholarship Council, China.

recently. The Gl_2 problem can be represented in LMI formulations (Gahinet *et al.*, 1995) and has been successfully applied to an active suspension system (Wang and Wilson, 2001). The Gl_2 approach has the potential to get solutions less conservative than those obtained via a H_∞ control synthesis approach whilst the computations involved in solving a Gl_2-optimization problem is more tractable than those required by the μ-optimization.

Like other LMI-based methodologies, the standard Gl_2 formulation relies on Lyapunov stability condition and the solution depends on the Lyapunov symmetric matrix P. Furthermore, in multi-objective synthesis, the Lyapunov matrices P in different LMI's are always assumed to be identical for the sake of solvability. Hence, it will inevitably introduce some new conservativeness to the whole optimal solution. To reduce such conservativeness in multi-objective problem, Geromel*et al.* (1998; 1999*b*; 1999*a*) extended the Lyapunov inequalities (called Lyapunov-shaping paradigm) by introducing a new stability condition. Using this new stability condition, the matrix G, possibly non-symmetric, decouples the Lyapunov matrices and the dynamical matrices of controller. Therefore, less conservative solutions are expected from the *G-shaping* paradigm (de Oliverira *et al.*, 1999*a*). This technique has been applied to many different control synthesis problems, such as H_2 and H_∞ optimization problems.

In this work, the *G-shaping* paradigm has been extended further to the Gl_2 optimization and pole placement problem. The later has been proven to be effective to improve the transient behavior of the closed-loop system.

The paper is organized as follows: In section 2, dynamics of an industrial nonlinear process, a evaporator system, is introduced. Then, section 3 discusses the extended Gl_2 controller design in details, which include performance weight selection and uncertainty modelling. In section 4, simulation results with the Gl_2 controller are compared with those obtained under other controllers. Finally, a brief summary of the proposed method is provided.

2. EVAPORATION PROCESS

A forced-circulation evaporator, described by Newell and Lee (1989), is shown in Figure 1. This is a typical nonlinear plant with potential model uncertainties. The system has been tested by many effective control strategies since it was published, such as PID, loop-shaping and model predictive Control (Newell and Lee, 1989; Samyudia *et al.*, 1995; Maciejowski, 2002).

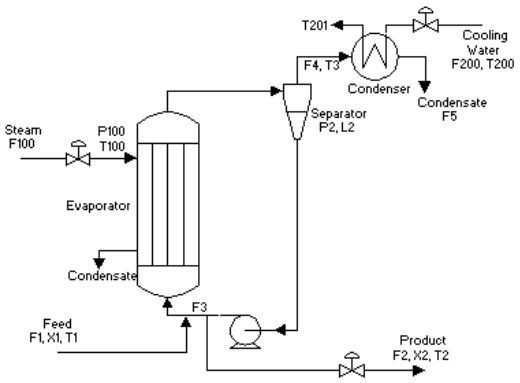

Fig. 1. Evaporator System

The nonlinear model of the plant is linearized at the nominal operating point as shown in Table 1, where S, M and D are variable abbreviations of State, Manipulated and Disturbance respectively. The corresponding linear state space representation is as follows:

$$\begin{bmatrix} \dot{L}_2 \\ \dot{X}_2 \\ \dot{P}_2 \end{bmatrix} = A \begin{bmatrix} L_2 \\ X_2 \\ P_2 \end{bmatrix} + B_1 \begin{bmatrix} P_{100} \\ F_2 \\ F_{200} \end{bmatrix} + B_2 \begin{bmatrix} F_1 \\ X_1 \\ T_1 \\ T_{200} \end{bmatrix}$$

where the matrices A, B_1 and B_2 are given as follows:

$$A = \begin{bmatrix} 0 & 0.0042 & 0.0075 \\ 0 & -0.1 & 0 \\ 0 & -0.0209 & -0.0558 \end{bmatrix}$$

$$B_1 = \begin{bmatrix} -0.0500 & -0.0019 & 0 \\ -1.2500 & 0 & 0 \\ 0 & 0.0096 & -0.0018 \end{bmatrix}$$

$$B_2 = \begin{bmatrix} 0.0467 & 0 & -0.0009 & 0 \\ 0.2500 & 0.5000 & 0 & 0 \\ 0.0164 & 0 & 0.0045 & 0.0360 \end{bmatrix}$$

Table 1. Description of Variables

Var	Description	Steady State	Type
L_2	Separator Level	1[m]	S
X_2	Product Composition	25%	S
P_2	Operating Pressure	50.5[kPa]	S
P_{100}	Steam Pressure	194.7[kPa]	M
F_2	Product Flow rate	2.0[kg/m]	M
F_{200}	Steam Flow rate	208.0[kg/m]	M
F_1	Feed Flow rate	10.0[kg/m]	D
X_1	Feed Composition	5.0%	D
T_1	Feed Temperature	40.0[^{o}C]	D
T_{200}	Cooling Water Temp	25.0[^{o}C]	D

The corresponding transfer functions of the system, G_p, from manipulated variables to outputs, and G_d, from disturbances to outputs, are denoted as:

$$G_p := \left[\begin{array}{c|c} A & B_1 \\ \hline I & 0 \end{array}\right], G_d := \left[\begin{array}{c|c} A & B_2 \\ \hline I & 0 \end{array}\right]$$

For the synthesis purpose, the input and output variables are scaled by divided by their steady-

state values. Then, the scaled transfer functions are $G_P = M_y^{-1} G_p M_u$ and $G_D = M_y^{-1} G_d M_d$, where M_y, M_u and M_d are diagonal scaling matrices with corresponding values shown in Table 1.

The control design objective is to achieve the following design specifications under disturbances and uncertainty.

- All controlled variables should be within 2% of the desired final value within 20 min of an upset and their maximum variations should be less than 100%.
- Variations in the manipulated variables should be less than 100% of their steady- state values.
- The above specifications should be satisfied for nonlinear model with reasonable disturbances and measurement noises.

3. EXTENDED GL_2 CONTROL DESIGN

A multi-objective optimization problem based on *G-shaping* is considered in this section. The aim is to compute a dynamical output feedback controller to meet the performance requirements specified as above. More precisely, these specifications are defined as sensitivity functions and their corresponding performance subject to uncertainties. Three weighting functions are to be chosen for this problem.

3.1 Performance Weight Selection

Applying the procedure presented in (Skogestad and Postlethwaite, 1996), the following performance weight for SISO system is considered:

$$w_e(s) = \frac{s/M + \omega_b}{s + \omega_b \sigma}$$

It specifies a minimum bandwidth ω_b, a maximum peak of the sensitivity S less than M, a steady state error less than $\sigma < 1$, and that at frequencies lower than the bandwidth the sensitivity is required to reduce by at least $20dB/dec$. In order to reduce the steady-state error to zero, $\sigma = 0$ is selected. Hence, the weight is actually a PI controller. For the sake of simplicity and tractable computation, the final performance weight matrix is to take the diagonal form as follows:

$$W_e(s) = \mathbf{diag}\{\frac{25s+25}{s+10^{-6}}, \frac{25s+25}{s+10^{-6}}, \frac{40s+10}{s+10^{-6}}\}$$

In the meantime, as usual, the control input sensitivity weight, $W_u(s)$ is simply selected as a constant matrix:

$$W_u(s) = \mathbf{diag}\{0.1, 0.1, 0.3\}$$

3.2 Uncertainty

Due to the nonlinearity and complicity of the actual plant, control design based on a simplified linear model has to consider model uncertainties. Therefore, an uncertainty weight to meet the robust control requirement is to be selected.

In this case study, it is assumed that the actual plant, $\tilde{G}_P$ is subject to a multiplicative unstructured input uncertainty, $\triangle^u$, weighted by W_{rob}, i.e.:

$$\tilde{G}_P := (I + W_{rob} \triangle^u) G_P, \ \|\triangle^u\|_\infty \leq 1$$

Normally, the uncertainty weight for SISO systems can take a simple form as follows:

$$w_{rob}(s) = \frac{\tau s + r_0}{(\tau / r_\infty)s + 1}$$

where r_0 is the relative uncertainty at steady state, $1/\tau$ is approximately the frequency where the relative uncertainty reaches 100%, and r_∞ is the magnitude of the weight at higher frequencies.

In the evaporation process, the main uncertainty is caused by nonlinearity rather than the neglected dynamics. By performing simulation with different set points and disturbances, the corresponding parameters of the weight are determined as $\tau = 20, r_0 = 8, r_\infty = 1$. It implies that in this design, 800% uncertainty of static gain is permitted. The final robust weight matrix is chosen as follows:

$$W_{rob} = \frac{(s+4)}{(s+0.5)} \mathbf{diag}\{2, 8, 4\}$$

By combining the above three weights, an augmented plant (see Figure 2) is defined as follows:

$$\begin{bmatrix} z_\triangle \\ \begin{bmatrix} z_e \\ z_u \end{bmatrix} \\ e \end{bmatrix} := G \begin{bmatrix} u_\triangle \\ \begin{bmatrix} r \\ d \\ n \end{bmatrix} \\ u \end{bmatrix}$$

where r, y and e represent system input, output and error(measurement output), u, z_e and z_u represent control output and controlled outputs, d and n are disturbance and measurement noise, and $u_\triangle$ and $z_\triangle$ are the output and input of uncertainty respectively.

In order to get a low order controller, disturbance d and measurement noise n in the above formulation will be ignored in the design. It will be shown that this ignorance has no noticeable effect on the final results in this case study. Thus, the augmented plant, G can be derived as:

$$G := \begin{bmatrix} 0 & 0 & W_{rob} \\ \begin{bmatrix} -W_e G_P \\ 0 \end{bmatrix} & \begin{bmatrix} W_e \\ 0 \end{bmatrix} & \begin{bmatrix} -W_e G_P \\ W_u \end{bmatrix} \\ -G_P & I & -G_P \end{bmatrix} \quad (1)$$

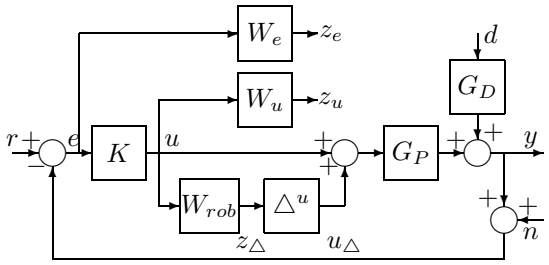

Fig. 2. Block Diagram Describing Weighted System with Multiplicative Uncertainty

3.3 Controller Synthesis

To use Gl_2 synthesis techniques, the augmented plant is represented in discrete state space form as follows:

$$\begin{aligned} x(k+1) &= Ax(k) + B_w w(k) + B_u u(k) \\ z(k) &= C_z x(k) + D_{zw} w(k) + D_{zu} u(k) \\ y(k) &= C_y x(k) + D_{yw} w(k) \end{aligned} \tag{2}$$

where, $x(k) \in \mathbb{R}^n$, $w(k) \in \mathbb{R}^{n_w}$, $u(k) \in \mathbb{R}^{n_u}$,$z(k) \in \mathbb{R}^{n_z}$ and $y(k) \in \mathbb{R}^{n_y}$ are discrete state, exogenous input, control input, controlled output and measurement output respectively. An output feedback controller $K(\zeta)$ defined in the following state-space form is to be designed:

$$\begin{aligned} x_c(k+1) &= A_c x_c(k) + B_c y(k) \\ u(k) &= C_c x_c(k) + D_c y(k) \end{aligned} \tag{3}$$

The closed-loop transfer function from w to z is defined as follows:

$$T_{zw}(\zeta) := \left[\begin{array}{c|c} \tilde{A} & \tilde{B} \\ \hline \tilde{C} & \tilde{D} \end{array}\right]$$

where the closed-loop system matrices are as follows:

$$\begin{aligned} \tilde{A} &:= \begin{bmatrix} A + B_u D_c C_y & B_u C_c \\ B_c C_y & A_c \end{bmatrix} \\ \tilde{B} &:= \begin{bmatrix} B_w + B_u D_c D_{yw} \\ B_c D_{yw} \end{bmatrix} \\ \tilde{C} &:= \begin{bmatrix} C_z + D_{zu} D_c C_y & D_{zu} C_c \end{bmatrix} \\ \tilde{D} &:= \begin{bmatrix} D_{zw} + D_{zu} D_c D_{yw} \end{bmatrix} \end{aligned}$$

In order to extend the Gl_2 optimization problem in (D'Andrea, 1999) to multi-objective synthesis based on G-shaping paradigm (Geromel *et al.*, 1998), the disturbance set $\mathcal{D}$ and criterion set $\mathcal{E}$ are reconstructed as follows

$$\mathcal{D} := \{d_k \in l_2 : \|d_k\| \le 1, k \in [1, m]\}$$

$$\mathcal{E} := \{z_l \in l_2 : \|z_l\| \le 1, l \in [1, n]\}$$

These sets result in the following inequalities

$$X := x_1 I_{d_1} \oplus x_2 I_{d_2} \oplus \cdots \oplus x_m I_{d_m} > 0, \sum_{k=1}^{m} x_k \le \mu \tag{4}$$

$$Y := y_1 I_{z_1} \oplus y_2 I_{z_2} \oplus \cdots \oplus y_n I_{z_n} > 0, \sum_{l=1}^{n} y_l \le \mu \tag{5}$$

where, $\oplus$ stands for direct sum of matrices, i.e.

$$A \oplus B = \begin{pmatrix} A & 0 \\ 0 & B \end{pmatrix}$$

I_{d_k} and I_{z_l} are the identity matrices with the same dimensions as $d_k d_k'$ and $z_l z_l'$ respectively. The Gl_2 optimization problem is to find a controller such that $\|T_{zw}(\zeta)\|_{Gl_2}^2 < \mu$, or equivalently, $\left\|X^{-1/2} T_{zw} Y^{-1/2}\right\|^2 < \mu$. Therefore, by new parameterization, the following central result to controller synthesis can be obtained (Yan and Cao, 2002).

Theorem 1. All controllers in the form (3) such that the inequality $\left\|X^{-1/2} T_{zw} Y^{-1/2}\right\|^2 < \mu$ holds are parameterized in (6) shown at the top of the next page.

In (6) the matrices $\Xi, L, \Pi, F, Q, R, S, J$ and the symmetric matrices P and H are the decision variables. The proofs of this and the coming theorem can be found in (Yan and Cao, 2002).

Remark 1. Given matrices $\Xi, L, \Pi, F, Q, R, S, J$ from the theorem, a feasible controller is available by choosing V and U nonsingular such that $VU = S - \Pi\Xi$ and calculating the following matrices in order

$$\begin{aligned} D_c &:= R \\ C_c &:= (L - R C_y \Xi) U^{-1} \\ B_c &:= V^{-1}(F - \Pi B_u R) \\ A_c &:= V^{-1}[Q - \Pi(A + B_u D_c C_y)\Xi] U^{-1} \\ &\quad - B_c C_y \Xi U^{-1} - V^{-1} \Pi B_u C_c \end{aligned} \tag{7}$$

Remark 2. The most important feature of this new framework is that the feasible controller (7) does not depend on any of the Lyapunov matrices P, J or H so that it can reduce the conservatism involved in standard multi-objective optimization problems and allow for more flexible and accurate specification of the closed loop behavior. Particularly, if $P = \Xi = \Xi'$, $J = S = I$, $H = \Pi = \Pi'$, it obviously encompasses the results obtained in (D'Andrea, 1999). Moreover, if the matrices X and Y in (6) are both set to μI, then the extended Gl_2 synthesis theorem is reduced to the standard H_∞ theorem. Therefore, the new framework is indeed a generalization of the standard Gl_2 framework.

$$\begin{pmatrix} P & J & A\Xi + B_u L & A + B_u R C_y & B_w + B_u R D_{yw} & 0 \\ (\cdot)' & H & Q & \Pi A + F C_y & \Pi B_w + F D_{yw} & 0 \\ (\cdot)' & (\cdot)' & \Xi + \Xi' - P & I + S' - J & 0 & \Xi' C_z' + L' D_{zu}' \\ (\cdot)' & (\cdot)' & (\cdot)' & \Pi + \Pi' - H & 0 & C_z' + C_y' R' D_{zu}' \\ (\cdot)' & (\cdot)' & (\cdot)' & (\cdot)' & X & D_{zw}' + D_{yw}' R' D_{zu}' \\ (\cdot)' & (\cdot)' & (\cdot)' & (\cdot)' & (\cdot)' & Y \end{pmatrix} > 0 \quad (6)$$

Normally, in order to improve the transient performance, a suitable closed-loop poles assignment is also necessary. Some closed-loop system poles constraints have been addressed recently in LMI form, and a general description for the continuous time system is presented in (Chilali and Gahinet, 1996). For a discrete time system, the following simple and effective constraint is defined to reduce the time response overshoot:

$$\mathcal{C}_{\mathcal{D}}(z_0, \rho) := \{\lambda \in \mathbb{C}, |\lambda + z_0| < \rho\} \quad (8)$$

Analogous to the above theorem, the extended poles placement LMI constraint for G-shaping is derived from (Yedavalli, 1993):

Theorem 2. (Poles Placement). All controllers in the form (3) such that poles of the closed-loop system satisfying (8) are parameterized by the following LMI

$$\begin{bmatrix} \rho P & \rho J & (A + z_0 I)\Xi + B_u L & A + B_u R C_y + z_0 I \\ (\cdot)' & \rho H & Q + z_0 S & \Pi(A + z_0 I) + F C_y \\ (\cdot)' & (\cdot)' & \rho\Xi + \rho\Xi' - \rho P & \rho I + \rho S' - \rho J \\ (\cdot)' & (\cdot)' & (\cdot)' & \rho\Pi + \rho\Pi' - \rho H \end{bmatrix} > 0$$

Combining these two theorems, the main results of the paper is stated as follows: The multi-objective Gl_2 synthesis problem is to find an optimal controller such that $\|T_{zw}(\zeta)\|_{Gl_2}^2 < \mu$ and the closed loop poles located inside the sub-region $\mathcal{C}_{\mathcal{D}}$.

This synthesis framework achieves the optimal performance of $T_{zw}(\zeta)$ while guaranteeing a certain level of robust stability and satisfactory of the system transient behavior. If the performance level μ is given, then the optimization problem is only to find the feasible solution under constraints stated in Theorems 1 & 2; otherwise, by absorbing μ into the corresponding two inequalities and casting it as another decision variable, the problem becomes a minimization problem with constraints. The programs for H_∞ and Gl_2 synthesis based on *G-shaping* have been developed in MATLAB using LMI Toolbox (Gahinet *et al.*, 1995).

4. SIMULATION RESULT COMPARISON

Based on the augmented plant of the evaporation process, the uncertainty block $\triangle$ for Gl_2(including two fictitious block) can be simply partitioned as follows:

$$\triangle := \triangle_{Gl_2} = \begin{bmatrix} \delta_{11} & \delta_{12} & \delta_{13} \\ \delta_{21} & \delta_{22} & \delta_{23} \end{bmatrix}$$

where $\delta_{ij} \in \mathbb{C}$, and $|\delta_{ij}| \leq 1, i \in \{1,2\}, j \in \{1,2,3\}$. Then the sets $\mathcal{D}$ and $\mathcal{E}$, related to the uncertainty $\triangle_{Gl_2}$ are defined as:

$$\mathcal{D} := \{d_i \in L_2 : \|d_i\| \leq 1, i \in \{1,2\}\}$$

$$\mathcal{E} := \{z_j \in L_2 : \|z_j\| \leq 1, j \in \{1,2,3\}\}$$

Consequently, inequality (4) and (5) become

$$X = x_1 I_3 \oplus x_2 I_3, Y = y_1 I_3 \oplus y_2 I_3 \oplus y_3 I_3$$

$$x_1 + x_2 \leq \mu, y_1 + y_2 + y_3 \leq \mu$$

where $x_i, y_j \in \mathbb{R}^+, i \in \{1,2\}, j \in \{1,2,3\}$. Then Gl_2 synthesis problem is simplified as:

$$\begin{aligned} \|T_{zw}\| &= \sup_{z \in \mathcal{E}, d \in \mathcal{D}} \langle z, T_{zw} d \rangle \\ &= \sup_{u_\triangle, r \in \mathcal{D}} \{\|T_{zw} u_\triangle\| + \|T_{zw} r\|\} \end{aligned}$$

Here we lump the weighted uncertainty outputs into $\|z_\triangle\|$, the weighted errors into $\|z_e\|$, the weighted control inputs into $\|z_u\|$, and the uncertainty inputs into $\|u_\triangle\|$, system set-points of L_2, X_2, P_2 into $\|r\|$. In μ-tools, δ_{12}, δ_{13} and δ_{21} are set 0. Moreover, some other partitions are also allowable in this framework. In fact, the 9 criterion elements and 6 disturbance elements can all be individual blocks, i.e., 'element by element'. Therefore, Gl_2 has more flexibility than H_∞ or μ-tools in dealing with uncertainty.

For the purpose of comparison, the above design problem is re-treated as a standard H_∞ (Scherer *et al.*, 1997) problem and a G-shaping H_∞ (de Oliverira *et al.*, 1999*a*) problem by constructing some fictitious performance blocks between z_e, z_u and r. Using the weights defined in section 3, two feasible nominal controllers K_1, K_2 and a robust optimal controller K_3 are obtained for standard H_∞, G-shaping H_∞ (GH_∞) and G-shaping Gl_2 optimization problems respectively.

In simulation, it is assumed that the setpoints of X_2 and P_2 are required to change from 25 to 15 and from 50.5 to 70, respectively while preserving L_2 unchanged for practical reason. Simultaneously, sinusoid disturbances with 20% magnitude variation are applied to both F_1 and X_1 with frequencies varying from 1 to 60Hz, a 20% step increase is applied to T_1 and 20% random

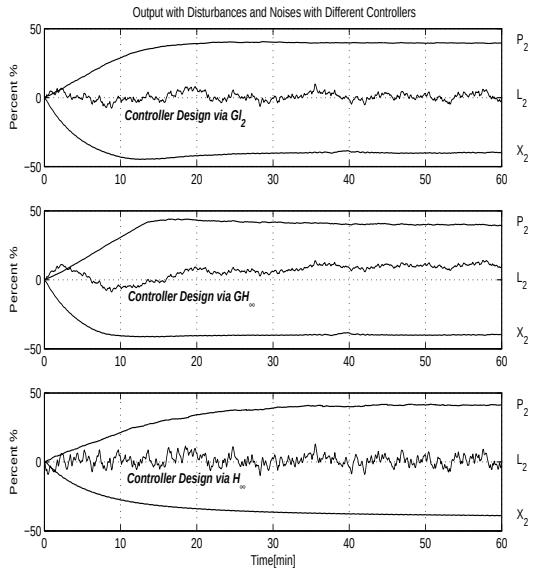

Fig. 3. Response to Step Changes in Setpoints

signal is applied to T_{200}. 20% random noises in all three measurement variables are also assumed.

Figure 3 illustrates the simulation results with different controllers. It demonstrates that the Gl_2 controller can produce better time performance than standard H_∞ and GH_∞ in this application. Under the same simulation condition, it is examined that PID control developed in (Newell and Lee, 1989) and Model predictive control developed in (Maciejowski, 2002) even cannot stabilize the system under such severe disturbance and noise conditions. It should be noted that if the μ-tools is applied to design this controller, it is quite difficult to choose properly scaled weight to get reasonable iterative results.

5. CONCLUSION

A new Gl_2 multiobjective robust control synthesis approach has been presented. It is jointly based on the work of Gl_2 by D'Andrea (1999) and G-shaping paradigm by Geromel *et al.* (1998). The new method can deal with disturbance and uncertainty simultaneously in a unified LMI form rather than $D-K$ iteration in μ synthesis. Based on G-shaping paradigm, the controller parameterization does not depend on the Lyapunov symmetric matrix P. It remains in the inequality just as an extra optimization variable. This results in a reduction of the conservativeness involved in a standard design framework. The freedom of design is improved as well. Although the approach presented in this paper is for discrete time system, it is easy to extend these concepts to continuous time system. Application to the evaporator system demonstrates that it can effectively improve the robustness and performance of a control system.

REFERENCES

Chilali, M. and P. Gahinet (1996). h_∞ design with pole placement constraints: An lmi approach. *IEEE Tran. on Automatic Control* **41**, 358–367.

D'Andrea, R. (1999). Generalised l_2 synthesis. *IEEE Transactions on Automatic Control* **44**, 1145–1156.

de Oliverira, M.C., J. Bernussou and J.C. Geromel (1999*a*). A new discrete time robust stability condition. *System and Control Letters* **37**, 261–265.

de Oliverira, M.C., J.C. Geromel and J. Bernussou (1999*b*). An lmi optimization approach to multiobjective controller design for discrete-time systems. In: *Proceedings of the 38th Conference on Decision and Control*. Phoenix, Arizona, USA.. pp. 3611–3616.

Gahinet, P., A.J. Laub A. Nemirovski and M. Chilali (1995). *LMI Control Toolbox, for Use with* MATLAB. The Math Works Inc.

Geromel, J.C., M.C. de Oliverira and L. Hsu (1998). Lmi characterization of structure and robust stability. *Linear Algera Appl.* **285**, 69–80.

Maciejowski, J.M. (2002). *Predictive Control with Constraints*. Pearson Education.

Newell, R.B. and P.L. Lee (1989). *Applied Process Control: A Case Study*. Prentice-Hall. Sydney.

Samyudia, R., P.L. Lee and I.T. Cameron (1995). A new approach to decentralised control design. *Chemical Engineering Science* **50**, 1695–1906.

Scherer, C., P. Gahinet and M. Chilali (1997). Multiobjective output-feedback control via lmi optimization. *IEEE Transactions on Automatic Control* **42**, 896–911.

Skogestad, S. and I. Postlethwaite (1996). *Multivariable Feedback Control-Analysis and Design*. John Willy & Sons. Baffins Lane, Chichester, England.

Toker, O. and H. Ozbay (1995). On the np-hardness of solving bilinear matrix inequalities and the simultanious stablization with static output feedback. In: *Proceedings of American Control Conference*. USA. pp. 2525–2526.

Wang, J. and D.A. Wilson (2001). Application of generalised l_2 synthesis to decoupled active suspension systems. In: *Proceedings of the American Control Conference*. Arlington, VA. pp. 25–27.

Yan, W.J. and Y. Cao (2002). An extention of Gl_2 synthesis optimization based on g-shaping paradigm. Submitted to ECC2003.

Yedavalli, R.K. (1993). Linear-quadratic control with stability degree constraint. *Systems & Control Letters* **21**, 261–265.

Nonlinear Control of a Fluid Catalytic Cracking Unit

Qing Yang, Shurong LI, Xuemin Tian

College of Information and Control Engineering, University of Petroleum (East China) ,
Dongying, Shandong, 257061, P.R. China. Email: lishuron@hdpu.edu.cn

Abstract- The dynamics of a fluid catalytic cracking unit (FCCU) is a typical nonlinear system. The purpose of this study is to develop a nonlinear control of a FCC unit via feedback linearization. Based on the mechanistic model of a FCC unit, a nonlinear controller is designed. The servo and tracking properties of the closed loop system are verified by simulation for a sample FCC unit. The simulation shows that the controller is valid and can be applied to practical FCC units.

Key words- nonlinear system, FCC unit, feedback linearization.

1. INTRODUCTION

The catalytic cracking has been one of the most important processes in petroleum refining. FCC units are known to be very difficult to modeling and control because of complex kinetics and dynamics of both cracking and coke burning reaction, multivariable character and the strong interaction between the riser and regenerator. Early papers on FCC unit modeling are mainly concerned with the reaction kinetics or steady-state process behavior. Weekman[9] proposed the three-lump and 10-lump cracking reaction models. Since Kurihara[6] firstly presented a dynamic model for bed-cracking type FCC unit in 1967, dynamic models for the riser-type FCC unit have been developed in recent years. Zheng [11, 12, 13] described a comprehensive dynamic model for side-by-side type FCC unit, including the reactor and the tow stage regenerator.

Most of controllers successfully used in FCC units are PID. Recently, model predictive control (MPC) based advanced control has been proposed and implemented in some plants [2, 8]. Since the dynamic model of the FCC unit is strongly nonlinear, the goal of the paper is to design a nonlinear controller based on the mechanistic model. By applying the theory of feedback linearization which developed mature in differential geometric control [3, 4, 5, 7], a nonlinear controller is synthesized. For a sample FCC unit, the simulation shows that the proposed controller assures not only the setpoint tracking but also the inner stability of the closed loop system.

2. FEEDBACK LINEARIZATION OF MIMO NONLINEAR SYSTEMS

Consider a following affine nonlinear system

$$\begin{cases} \dot{X} = f(X) + g_1(X)u_1 + g_2(X)u_2 \\ \qquad + \cdots + g_m(X)u_m \\ y_1(t) = h_1(X) \\ \cdots\cdots \\ y_m(t) = h_m(X) \end{cases} \tag{2.1}$$

where $X \in R^n$ is the state vector; $f(X)$ and $g_i(X)$ are n dimension vector fields; u_i are

the control variables; $y_i(t)$ are the controlled variable; $h_i(X)$ is a scalar function of X, $i=1,2,\cdots,m$. Assume X_0 is an equilibrium point, i.e. $f(X_0)=0$, $h_1(X_0)=h_2(X_0)=\cdots=h_m(X_0)=0$.

If system (2.1) has relative degree $r=\{r_1,r_2,\cdots,r_m\}$ [7], where r satisfies $r_1+r_2+\cdots+r_m=r\le n$, following nonlinear coordinate transformation can be acquired:

$$z_1^1=h_1(X),z_2^1=L_fh_1(X),\cdots,z_{r_1}^1=L_f^{r_1-1}h_1(X)$$
$$\cdots$$
$$z_1^m=h_m(X),z_2^m=L_fh_m(X),\cdots,z_{r_m}^mL_f^{r_m-1}h_m(X)$$

If $r\ne n$, the other $n-r$ nonlinear coordinate transformation should be chosen:

$$z_{r+1}=\eta_1(x),\cdots,z_n=\eta_{n-r}(x)$$

If the Jacobian matrix $\frac{\partial Z(X)}{\partial X}$ is nonsingular at $X=X_0$, following system can be obtained

$$\begin{cases}\dot z_j^i=z_{j+1}^i,\\ \dot z_{r_i}^i=b^i(z,\eta)+\sum_{k=1}^m a_k^i(z,\eta)u_k=v_i\\ \dot\eta=q(z,\eta)+\sum_{k=1}^m p_k^i(z,\eta)u_k\\ y_i=z_1^i\end{cases}$$

where, $i=1,2,\cdots,m$ and $1\le j\le r_i-1$

Since *A(z)* is nonsingular, solved the following equation

$$\begin{bmatrix}\dot z_{r_1}^1\\ \vdots\\ \dot z_{r_m}^m\end{bmatrix}=\begin{bmatrix}b_1(z)\\ \vdots\\ b_m(z)\end{bmatrix}+\begin{bmatrix}a_1^1(z) & a_2^1(z) & \cdots & a_m^1(z)\\ \vdots & \vdots & \cdots & \vdots\\ a_1^m(z) & a_2^m(z) & \cdots & a_m^m(z)\end{bmatrix}\begin{bmatrix}u_1\\ \vdots\\ u_m\end{bmatrix}=\begin{bmatrix}v_1\\ \vdots\\ v_m\end{bmatrix}$$

can obtain *u*

$$u=A^{-1}(z)(-b(z)+v)$$

If the zero dynamics of the system $\dot\eta=q(0,\eta)+p(0,\eta)[-A^{-1}(0,\eta)b(0,\eta)]$ is asymptotically stable, let $v_i=(s^{ri}+c_{ri-1}s^{ri-1}+\cdots+c_1s+c_0)z_1^i,i=1,\cdots,m$. Here the c_i are chosen so that $s^{ri}+c_{ri-1}s^{ri-1}+\cdots+c_1s+c_0$ is a Hurwitz polynomial. Then, an asymptotically stable closed loop system is obtained.

3. FEEDBACK LINEARIZATION OF A FCC UNIT

3.1 Process model of a FCC unit

Fig.1. shows the reactor and regenerator part of a FCC unit. The feed injected into the reactor riser, where it mixes with hot regenerated catalyst and vaporizes. The hot catalyst provides the heat of vaporization and the heat of reaction. As a result of the cracking reactions, a carbonaceous material (coke) is deposited on the surface of the catalyst. The catalyst and gas are separated in the settler. Then spent catalyst is transported from the reactor to the regenerator. In the regenerator, catalyst is fluidized with air flow injected from the bottom of the regenerator. Carbon and hydrogen on the catalyst react with oxygen to produce carbon monoxide, carbon dioxide and water. Regenerated catalyst flows into the reactor riser.

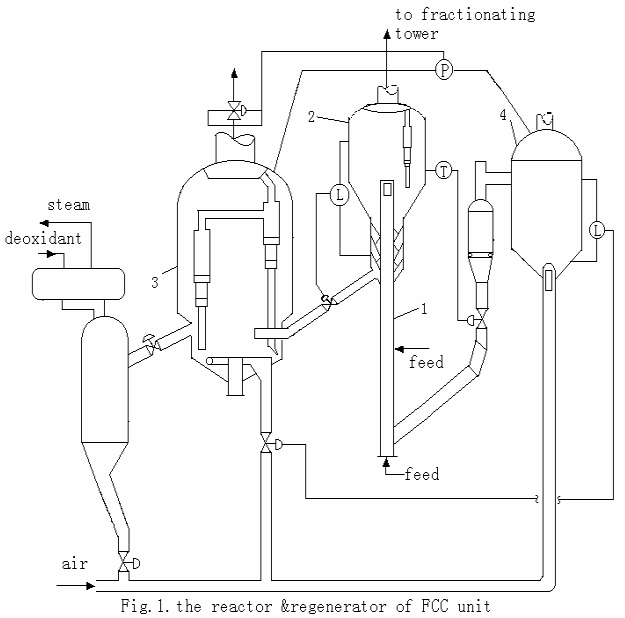

Fig. 1. the reactor &regenerator of FCC unit
1. reator 2. settler 3. the first stage of regenerator 4. the second stage of regenerator

Manipulated variables are mass flow rate of

the catalyst entering the riser (R_C), mass flow rate of the spent catalyst entering the spent catalyst transport line (R_{CS}) and mass flow rate of the regenerated catalyst in the first stage of regenerator (R_{CG1}).Controlled variables are temperature of reactor riser outlet (T_{RA2e}), inventory of catalyst in the settler (H_S) and inventory of catalyst in the second stage of regenerator (H_{GC2}).

Based on the references [11] [12] and [13], a dynamic mathematical model of a FCC unit can be obtained

$$\frac{dT_{RA1e}}{dt} = -\frac{1}{S_{T1}} * \frac{1}{1+\prod_1} (\mathrm{T_{RA1e}} - \mathrm{T_{RA1i}}) - \frac{1}{S_{T1}} * \frac{1}{1+\prod_1} \wedge_1 \frac{R_C}{R_{O1}} \mathrm{C_{CA1e}} \quad (3.1.1)$$

$$\frac{dT_{RA2e}}{dt} = -\frac{1}{S_{T2}} * \frac{1}{1+\prod_2} (\mathrm{T_{RA2e}} - \mathrm{T_{RA2i}}) - \frac{1}{S_{T1}} * \frac{1}{1+\prod_1} \wedge_2 \frac{R_C}{R_{O2}} (\mathrm{C_{CA2e}} - \mathrm{C_{CA1e}}) \quad (3.1.2)$$

$$\frac{dH_S}{dt} = R_{CS} - R_C \quad (3.1.3)$$

$$\frac{dH_{GC1}}{dt} = R_{CS} - R_{CG1} \quad (3.1.4)$$

$$\frac{dC_{G1}}{dt} = \frac{1}{H_{GC1}}[R_{CS}(C_S - C_{G1}) - \frac{R_{A1}}{\nu_{OC}}(0.21 - O_{FG1})] \quad (3.1.5)$$

$$\frac{dT_{RG1}}{dt} = \frac{1}{H_{GC1}C_{PC}}[\frac{R_{A1}}{\nu_{OC}}(0.21 - O_{FG1})(\Delta H_{CB}) - R_{CS}C_{PC}(T_{RG1} - T_S) - R_{A1}C_{PA}(T_{RG1} - T_A)] \quad (3.1.6)$$

$$\frac{dH_{GC2}}{dt} = R_{CG1} - R_{CG2} \quad (3.1.7)$$

$$\frac{dC_{G2}}{dt} = \frac{1}{H_{GC2}}[R_{CG1}(C_{G1} - C_{G2}) - \frac{R_{A2}}{\nu_{OC}}(0.21 - O_{FG2})] \quad (3.1.8)$$

$$\frac{dT_{RG2}}{dt} = \frac{1}{H_{GC2}C_{PC}}[\frac{R_{A2}}{\nu_{OC}}(0.21 - O_{FG2})(\Delta H_{CB}) - R_{CS}C_{PC}(T_{RG2} - T_{RG1}) - R_{A2}C_{PA}(T_{RG2} - T_A)] \quad (3.1.9)$$

The physical significance of each variable shows in appendix A. the detailed expressions of Π, Λ, $\mathrm{C_{CAe}}$, $\mathrm{T_{RAi}}$ and $\mathrm{O_{FG}}$ are shown in references [11] [12] and [13].

3.2 Design of the controller

Before designing the controller, we assumpt that the total inventory of catalyst is a constant; that is to say, the losing of catalyst is neglected.

Then we can draw that the inventory of catalyst in the first stage of regenerator H_{GC1} can be computed by using the following equation:

$$H_{GC1} = H - H_S - H_{GC2}$$

where H is the total inventory of catalyst.

Moreover, because of the characteristics of catalyst transport line, the system has another two qualities:

1: Mass flow rate of the catalyst entering the riser R_C, mass flow rate of the spent catalyst entering the spent catalyst transport line R_{CS}, mass flow rate of the regenerated catalyst in the first stage of regenerator R_{CG1} and mass flow rate of the regenerated catalyst in the second stage of regenerator R_{CG2} are all constrained:

$0 < R_C, R_{CS}, R_{CG1}, R_{CG2} < R$

2: mass flow rate of the regenerated catalyst in the second stage of regenerator is equal to mass flow rate of the catalyst entering the riser:

$$R_{CG2} = R_C$$

It shows that the reactor and regenerator part of a FCC unit is a nine stage nonlinear system with three inputs and three outputs, but it is not an affine system. We introduce a new variable $u_1$defined as below

$$\dot{R}_C = u_1$$

Let, $R_{CS} = u_2$; $R_{CG1} = u_3$; $T_{RA1e} = x_1$; $T_{RA2e} = x_2$; $R_C = x_3$; $H_s = x_4$; $C_{G1} = x_5$; $T_{RG1} = x_6$; $H_{GC2} = x_7$; $C_{G2} = x_8$; $T_{RG2} = x_9$.

Assume that some disturbance exists such as mass flow rate of feed R_O , temperature of feed T_{Oi} and pressure of regenerator P_{RG} . Then, an

affine system can be obtained as follows

$$\begin{cases} \dot{x}_1 = f_1(x_1, x_3) + d_1 \\ \dot{x}_2 = f_2(x_1, x_2, x_3) + d_2 \\ \dot{x}_3 = u_1 \\ \dot{x}_4 = x_3 - u_2 \\ \dot{x}_5 = f_5(x_4, x_5, x_6, x_7) + g_5(x_4, x_5, x_7)u_2 + d_5 \\ \dot{x}_6 = f_6(x_4, x_5, x_6, x_7) + g_6(x_4, x_6, x_7)u_2 + d_6 \\ \dot{x}_7 = u_3 - x_3 \\ \dot{x}_8 = f_8(x_7, x_8, x_9) + g_8(x_5, x_7, x_8)u_3 + d_8 \\ \dot{x}_9 = f_9(x_7, x_8, x_9) + g_9(x_6, x_7, x_9)u_3 + d_9 \\ Y = [x_2, x_4, x_7]^T \end{cases} \tag{3.2.1}$$

The relative degree of system (3.2.1) is $\{r_1, r_2, r_3\} = \{2,1,1\}$.

Let, $z_1 = x_2, z_2 = L_f x_2, z_3 = x_4, z_4 = x_7$, $z_\eta = \{\eta \mid \eta \in x \quad \eta \neq x_2, x_3, x_4, x_7\} \subset R^{n-4}$. Then, system (3.2.1) can be changed to:

$$\begin{cases} \dot{z}_1 = z_2 + d_1 \\ \dot{z}_2 = v_1 \\ \dot{z}_3 = v_2 \\ \dot{z}_4 = v_3 \end{cases} \tag{3.2.2a}$$

$$\dot{\eta} = q(\xi, \eta) + w_\eta d_\eta \tag{3.2.2b}$$

$$[y_1, y_2, y_3]^T = [z_1, z_3, z_4]^T \tag{3.2.2c}$$

The feedback linearization controller of system (3.2.2) is:

$$u_1 = \frac{v_1 - (\partial f_2 / \partial x_1) f_1 - (\partial f_2 / \partial x_2) f_2}{\partial f_2 / \partial x_3};$$

$u_2 = x_3 - v_2$; $u_3 = x_3 + v_3$,

where,

$v = -[\alpha_{11}(z_1 - y_{1d}) + \alpha_{12} z_2 \quad \alpha_2(z_3 - y_{2d}) \quad \alpha_3(z_4 - y_{3d})]^T$,

$\alpha_{11}, \alpha_{12}, \alpha_2, \alpha_3 > 0$ and y_{1d}, y_{2d}, y_{3d} are desired outputs.

If (3.2.2b) is asymptotically stable at the steady point, the output of the closed loop system can asymptotically track the desired output [5].

3.3 The verification of stability of zero dynamics

Based on the above analysis, if the zero dynamics of system (3.2.2b) is asymptotically stable at the steady point, the closed loop system is stable.

Because zero dynamics of this system is very complex, proving its stability by using Lyapunov function is difficult. Therefore, we prove zero dynamics stability by computing the eigenvalues of the Jacobian matrix of zero dynamics (3.2.2b) at some steady point. If the eigenvalues are in the left-half plane, the zero dynamics (3.2.2b) is asymptotically stable in the neighborhood of the steady point. We choose several steady points, and calculate the Jacobian matrix of system (3.2.2b) in each steady state. The results show that the eigenvalues of each Jacobian matrix are in the left-half plane. Therefore, the stability of the closed loop system can be assured.

4. RESULTS OF SIMULATION

The values of the variables in steady states are shown in appendix 2. In the simulation, the desired outputs: temperature of reactor riser outlet T_{RA2e}, inventory of catalyst in the settler H_S and inventory of catalyst in the second stage of regenerator H_{GC2} are changed from [800.5754,990,32.662] to [790,1000,260]. Fig.2, Fig.3 and Fig.4 show the comparison results of tracking reference trajectories of outputs by using feedback linearization and PID controllers respectively. It is shown that the controller designed by using feedback linearization makes the closed loop have better properties than a PID controller does. (the outputs of feedback linearization: —, the outputs of PID: ----). Fig.5 shows the capability of rejecting disturbance of feedback linearization controller.

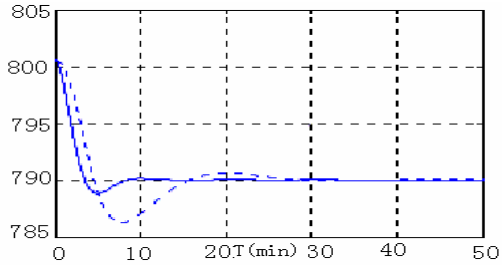

Fig.2. Temperature of riser outlet

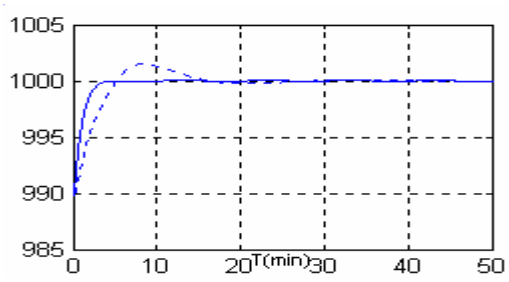

Fig.3. Inventory of catalyst in settler

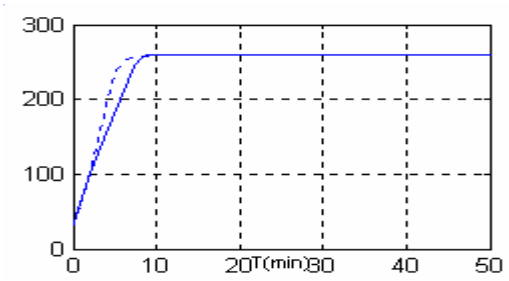

Fig.4. Inventory of catalyst in the second stage of regenerator

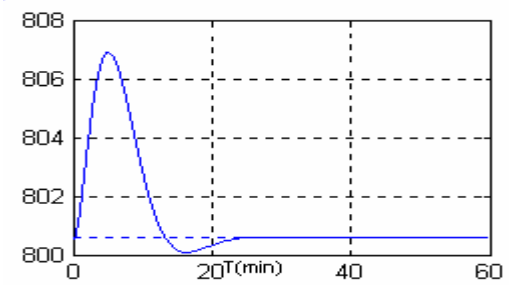

Fig.5. Temperature of riser out let when flow rate of feed reduce 5%

To show the stability of the closed loop system, the Jacobian matrix of zero dynamics of system in the steady point (appendix B) is computed as follows:

$$\begin{bmatrix} -17.3 & 0 & 0 & 0 & 0 \\ 0 & -0.3 & -8.6\times10^{-62} & 0 & 0 \\ 0 & -1.1\times10^{-52} & -0.3 & 0 & 0 \\ 0 & 5.7 & 0 & -2.8\times10^{3} & -1.8\times10^{-15} \\ 0 & 0 & 5.7 & 1.4\times10^{-19} & -5.7 \end{bmatrix}$$

The eigenvalues of the Jacobian matrix are-17.3, -5.7, -0.3, -2.8*10^3 and -0.3, which are in the left-half plane. Therefore, the closed loop system is asymptotically stable.

Fig.6, Fig.7 and Fig.8 show the simulation results of the temperature of the second feed inlet, the temperature of the second stage of regenerator and the mass fraction of coke in regenerated catalyst at the second stage of regenerator. The results validate the stability of zero dynamics.

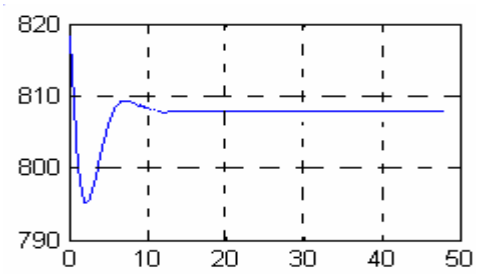

Fig.6. Temperature of the second feed inlet of riser

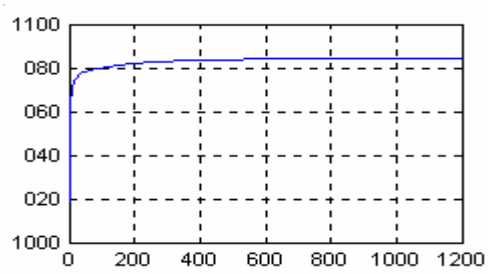

Fig.7. Temperature of the second stage of regenerator

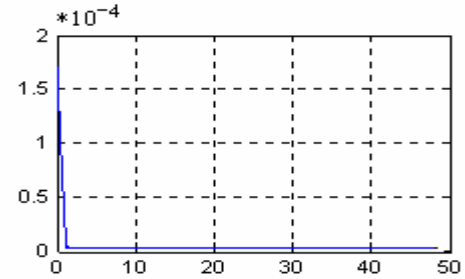

Fig.8. Mass fraction of coke in catalyst at the second stage of regenerator

5. CONCLUSIONS

In this paper, by designing a nonlinear controller of a FCC unit, we can draw the following conclusions.

1. The feedback linearization method can be used in the controller design of a FCC unit. The simulation results show that the proposed nonlinear controller can guarantee not only the closed loop stability, but also setpoint tracking.

2. The controller can effectively reject some disturbance which shows the robustness of the controller. When some disturbance, such as R_O, T_{Oi} and P_{RG}, exist in the system, the controller can still assure the closed loop stability.

The above analysis demonstrates that the controller proposed in this paper can be applied in practical plants.

APPENDIX A. NOMENCLATURE

Riser

C_{CA}	Mass fraction of reactive carbon in catalyst, [0-1]
C_G	Mass fraction of carbon in regenerated catalyst
C_S	Mass fraction of carbon in spent catalyst
ΔH_{CR}	Heat of reaction J/Kg catalyst
P_{RA}	Pressure of reactor Pa
R	Universal gas constant 8.315J/mol*K
R_C	Mass flow rate of catalyst Kg/S
R_O	Mass flow rate of feed Kg/S
R_W	Mass flow rate of vapor Kg/S
S_T	Feed space time S
T_{RA}	Temperature of reactor K
t	Time S
Y_A	Mass fraction of unconverted hydrocarbons
H_S	Inventory of catalyst in settler, Kg

Regenerator

C_G	Mass fraction of carbon in regenerated catalyst
C_S	Mass fraction of carbon in spent catalyst
C_{PA}	Specific heat of air KJ/(Kg*K)
C_{PC}	Specific heat of catalyst J/Kg*K
H_{GC}	Inventory of catalyst in regenerator, Kg
ΔH_{CB}	Heat of carbon burning , KJ/Kg carbon
O_{FG}	Mole fraction of oxygen in flue gas [0-1]
R_A	Volume flow rate of flue gas, Nm^3/h
R_{CG}	Mass flow rate of regenerated catalyst
R_{CS}	Mass flow rate of spent catalyst
T_A	Temperature of air at regenerator inlet
T_A	Temperature of air
T_{RG}	Temperature of regenerator
T_S	Temperature of spent catalyst
ν_{OC}	Stoichiometric coefficient, Nm^3oxygen/Kg carbon

APPENDIX B

The values of the variable in steady states are shown as follow. The definition of symbols which were not shown in this paper can be found in reference [11], [12] and [13].

K_{A0}=199.476	K_{C0}=0.04916	$K_{\varphi 0}$=0.05652
E_A=79100	E_C=41300	P_{RA}=101325
R=8.315	V_{r1}=14.2545	V_{r2}=25.7634
V_{l1}=5.50128	V_{l2}=6.93312	ρ_{Oi}=0.8 ρ_L=2050
R_O=250	R'_O=50	R_C=1578.085
R_{w1}=16	R_{w2}=3	T_{o1i}=473.15
T_{c1i}=1012.15	T_{w1i}=523.15	T_{o2i}=606.65
T_{w2i}=523.15	ΔH_{CR}=257200	ΔH_V=40000
C_{po}=800	C_{pc}=260	C_{pw}=200
C_{pl}=0.21	P_a=2.8	n=2
K_{R0}=83600000	E_{CB}=50	K_{DO}=1.43

REFERENCES

1. Ali, H., & Rohani, S. Dynamic modeling and simulation of a riser-type fluid catalytic cracking unit. *Chemical Engineering Technology, 1997, 20, 118-130.*
2. C. Loeblein & J. D. Perkins. Structural Design for on-line process optimization: II. Application to a simulated FCC.
3. Costas Kravaris, Jeffery C.Kantor. Geometric Methods for Nonlinear Process Control. 1.Background. *Ind.Eng.Chem.Res.1990,29, 2295 -2310*
4. Costas Kravaris, Jeffery C.Kantor. Geometric Methods for Nonlinear Process Control. 2. Controller Synthesis. *Ind.Eng.Chem.Res. 1990,29, 2311-2323*
5. Isidori, A. Nonlinear Control Systems, 2nd ed., *Springer-Verlag, New York, 1989.*
6. Kurihara, H., phD. Theis *MIT*, ESL-R-309, *1967.*
7. Lu Qiang & Sun Yuanzhang. Nonlinear Control of Electric Power System. *Science Publishing Company. 1993.*
8. R.M.Ansari, M.O.Tade. Constrained nonlinear multivariable control of a fluid catalytic cracking process. *Journal of Process Control, 2000, 10, 539-555*
9. Weekman Jr.V., W. *IEC/PDD.,7(1).1986,90.*
10. Y.-Y. Zheng. Dynamic Model And Simulation of a Catalytic Cracking Unit. *Computers & Chemical Engineering, 1994, Vol. 18, No. 1, P39-44.*
11. Zheng Yuanyang. Dynamic Model of Catalytic Cracking Unit I. *Petroleum Refining. 1986(2),P23-30.*
12. Zheng Yuanyang & Gao Shaoli. Dynamic Model of Catalytic Cracking Unit Ⅱ. *Petroleum Refining. 1986(4), P67-71*
13. Zheng Yuanyang & Gao Shaoli. Dynamic Model of Catalytic Cracking UnitⅢ. *Petroleum Refining. 1986(5), P45-49*

ESTIMATOR DESIGN WITH PLS MODEL FOR CONSISTENT CONTROL OF REFINERY MAIN FRACTIONATORS

Dante Pastore * **Alessandro Brambilla** * **Gabriele Pannocchia** *,[1]

* *Department of Chemical Engineering – University of Pisa*
Via Diotisalvi 2, 56126 Pisa (Italy)

Abstract: In this paper the problem of designing product quality inferentials for refinery main fractionations is addressed by using the PLS regression. A simulated crude distillation unit is chosen as case study, and several linear steady-state estimators are designed and compared in terms of accuracy and consistency, i.e. the estimator ability of guaranteeing low closed-loop offset. The paper shows the importance of the auxiliary measurement choice in order to build an effective inferential control scheme. Moreover, it shows that the use of only temperature measurements is not sufficient to guarantee an acceptable estimator performance. Additional measurements as the operating pressure and internal flows have been used to improve the estimator accuracy and consistency.

Keywords: distillation control, estimator, consistency, inferential

1. INTRODUCTION

Product quality control is an important and difficult issue in many chemical applications and in particular in refinery main fractionators because of the effect of these units on the quality of final commercial products and on the efficiency of downstream operations. For such processes on-line quality analyzers are not widely used because they are expensive, because they require frequent maintenance work and because, for some properties, they are not available. Moreover, on-line analyzers suffer from large time delays which would make the product quality control a difficult task. Indeed, a common alternative is to use some auxiliary measurements (often tray temperatures) to infer the product properties, thus building an inferential control scheme. The issue of measurement selection is of crucial importance for the effectiveness of an estimator, and it has been the subject of extensive research in the chemical engineering community (Joseph and Brosilow, 1978; Morari and Stephanopoulos, 1980; Yu and Luyben, 1987; Mejdell and Skogestad, 1991).

In this work product quality estimators are investigated for a crude distillation unit (which is one of the most common main fractionators present in oil refineries) using the PLS regression technique. Comparisons among different linear steady-state estimators in terms of accuracy and achievable control performance are presented. To this aim the concept of estimator closed-loop consistency (Pannocchia and Brambilla, 2002) is used, and results show that estimators "apparently" well designed (i.e. in terms of accuracy) should not be used in an inferential control scheme because they would lead to improper control actions with significant closed-loop offset in the presence of disturbances and/or set-point changes.

2. BASIC BACKGROUND CONCEPTS

2.1 *PLS regression*

PLS is a multivariate regression technique that can easily handle large numbers of noisy and correlated data sets, and it is based on the extraction of a number of *latent variables* which are linear combinations of the original predictor variables. PLS has been extensively applied in chemometrics (see e.g. (Wold *et al.*, 2001*b*) and references therein) and, more recently, in the area of process engineering (Mejdell and Skogestad, 1991; Kresta *et al.*, 1994; Kano *et al.*, 2000);

[1] Corresponding author. Email: pannocchia@ing.unipi.it, Fax: +39 050 511266.

several extensions of PLS have been proposed during the last years (see e.g. (Wold *et al.*, 2001*a*) and references therein).

Linear PLS seeks a relation between the auxiliary variables $x \in \mathbb{R}^m$ and the response (dependent) variables $y \in \mathbb{R}^p$ of the type:

$$\hat{y} = Kx \ , \tag{1}$$

in which $\hat{y} \in \mathbb{R}^p$ is the $y-$estimate and $K \in \mathbb{R}^{p \times m}$ is the estimator gain. Notice that both the auxiliary variables and the response variables are centered around a reference (mean) value, so that no constant bias term appears in (1). Given a set of n training runs, i.e. n vectors x and the corresponding n vectors y, the matrices X and Y are built by stacking the corresponding x and y vectors as rows. Usually, each variable (i.e. each column of X and Y) is scaled to unit variance. Then, PLS generates a "few" (k in number) $X-$scores as a linear combination of the original variables:

$$T = XW \ , \tag{2}$$

in which $T \in \mathbb{R}^{n \times k}$ is the $X-$score matrix and $W \in \mathbb{R}^{m \times k}$ is an appropriate weight matrix. These weights are computed so that each of them maximizes the covariance between the response variables and the $X-$scores. The $X-$scores are, multiplied by an appropriate loading matrix $P \in \mathbb{R}^{m \times k}$, good "summaries" of X, that is:

$$X = TP^T + E \ , \tag{3}$$

in which $E \in \mathbb{R}^{n \times m}$ contains the $X-$residuals. Then, a linear regression model for Y is obtained as:

$$Y = TQ^T + F = XWQ^T + F \ , \tag{4}$$

in which $Q \in \mathbb{R}^{p \times k}$ is an appropriate matrix and $F \in \mathbb{R}^{n \times p}$ contains the $Y-$residuals. Finally, the PLS regression estimates can be written as:

$$\hat{Y} = XK^T \ , \tag{5}$$

in which the estimator gain is given by

$$K = QW^T \ . \tag{6}$$

Several PLS algorithms exist in literature (Wold *et al.*, 2001*b*) and the following by de Jong (1993) is used in this work.

Algorithm 1. (SIMPLS).
For each $h = 1, \ldots, k$ (where $A_1 = \Theta^T Y$, $M_1 = \Theta^T \Theta$, $C_1 = I$), repeat the following steps:

(1) compute q_h, the dominant eigenvector of $A_h^T A_h$,
(2) set $w_h = A_h q_h$, $c_h = w_h^T M_h w_h$, $w_h \leftarrow w_h / \sqrt{c_h}$, and store w_h into W as a column,
(3) set $p_h = M_h w_h$, and store p_h into P as a column,
(4) set $q_h = A_h^T w_h$, and store q_h into Q as a column,
(5) set $v_h = C_h p_h$ and $v_h \leftarrow v_h / \|v_h\|_2$,
(6) set $C_{h+1} = C_h - v_h v_h^T$ and $M_{h+1} = M_h - p_h p_h^T$,
(7) set $A_{h+1} = C_{h+1} A_h$.

Multivariate techniques as PLS can also be used to select a smaller number of auxiliary variables to be used in the estimator. In this work, several tray temperatures are used to estimate the product quality properties of interest (see Section 3), and the location choice of such temperatures is based on the method discussed in (Mejdell and Skogestad, 1991, Sec. 5.6). However, it is important to remark that several engineering considerations specific of refinery main fractionators will be made to exclude some trays.

An important issue in PLS is the determination of the number of latent variables to use. To this aim, the so-called "Explained Variance" (EV) is introduced. Let $y_{i,j}$ be the actual value of the $j-$th response variable in the $i-$th calibration run, and let $\hat{y}_{i,j}(k)$ be the corresponding estimate obtained by the PLS estimator with k latent variables. Then, the "Mean Square Error" (MSE) for the $j-$th response variable is given by:

$$\mathrm{MSE}_j(k) = \frac{1}{n} \sum_{i=1}^{n} (y_{i,j} - \hat{y}_{i,j}(k))^2 \ , \tag{7}$$

and the Explained Variance (EV) for the j-th product composition is

$$\mathrm{EV}_j(k) = 100 \left(1 - \frac{\mathrm{MSE}(k)}{\mathrm{MSE}(0)} \right) \ . \tag{8}$$

Typically, one increases the number of latent variables k until the increment in EV, i.e. $\mathrm{EV}(k+1) - \mathrm{EV}(k)$, is not significant (say less than 1-2%). In fact, if a latent variable which gives a small increment in the explained variance is used, the estimator accuracy does not improve significantly while the estimator becomes sensitive to data errors aligned with the direction of this latent variable, and the estimator prediction ability deteriorates. See e.g. (Wold *et al.*, 2001*b*, par. 3.8) for a detailed discussion on methods for choosing the number of latent variables.

2.2 *Estimator consistency*

Usually, the estimator is designed to fit the training data reasonably well and it is validated with additional (historical) data (as well as with real time plant data). After this stage, the estimator is inserted into the control loop, and no implications on the control performance, e.g. about the steady-state offset, are evaluated at the estimator design stage. The underlying assumption is that if an estimator fits the data sufficiently well the corresponding inferential control scheme will perform satisfactorily, as well. However, in general this is incorrect.

In order to address this "myth" Pannocchia and Brambilla (2002) recently introduced the concept of estimator consistency, which is the ability of an estimator to guarantee low steady-state offset in the unmeasured controlled variables in the presence of disturbances (and/or setpoint changes). It is shown that the estimator consistency is not necessarily related to its accuracy, and it is shown how the steady-state offset is related to the estimator consistency. The problem of closed-loop consistency arises even in single-input single-output (SISO) systems and it is more dramatic for multi-input multi-output (MIMO) systems, as the

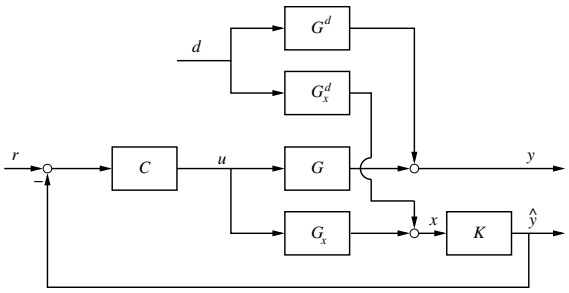

Fig. 1. Inferential control scheme

process studied in this work. This concept is quantified through the introduction of an appropriate consistency measure, which is briefly recalled.

Consider the generic inferential control scheme reported in Fig. 1, in which $u \in \mathbb{R}^p$ is the manipulated variable, $y \in \mathbb{R}^p$ is controlled variable (unmeasurable), $x \in \mathbb{R}^m$ is the auxiliary variable (measurable), $\hat{y} \in \mathbb{R}^p$ is the estimate of the controlled variable, and $d \in \mathbb{R}^q$ is the disturbance input. Notice that the feedback controller C operates on the estimate of the controlled variable, i.e. on $\hat{y}$. For a generic disturbance $d \neq 0$ (assuming $r = 0$), the consistency matrix $\xi = \{\xi_{i,j}\}$ is defined as (Pannocchia and Brambilla, 2002):

$$\xi_{i,j} = \frac{\left(\frac{\partial u_i}{\partial d_j}\right)_{\hat{y}=0}}{\left(\frac{\partial u_i}{\partial d_j}\right)_{y=0}} = \frac{\left\{\begin{array}{c}\text{variation of } u_i \text{ when} \\ \text{rejecting } d_j \text{ on } \hat{y}\end{array}\right\}}{\left\{\begin{array}{c}\text{variation of } u_i \text{ when} \\ \text{rejecting } d_j \text{ on } y\end{array}\right\}} \quad (9)$$

Similarly, for a generic setpoint change $r \neq 0$ (assuming $d = 0$) the consistency matrix $\varphi = \{\varphi_{i,j}\}$ is defined as:

$$\varphi_{i,j} = \frac{\left(\frac{\partial u_i}{\partial r_j}\right)_{\substack{\hat{y}_j = r_j \\ \hat{y}_{l\neq j}=0}}}{\left(\frac{\partial u_i}{\partial r_j}\right)_{\substack{y_j = r_j \\ y_{l\neq j}=0}}} = \frac{\left\{\begin{array}{c}\text{variation of } u_i \text{ to bring} \\ \hat{y}_j \text{ to } r_j \text{ with } \hat{y}_{l\neq j} = 0\end{array}\right\}}{\left\{\begin{array}{c}\text{variation of } u_i \text{ to bring} \\ y_j \text{ to } r_j \text{ with } y_{l\neq j} = 0\end{array}\right\}} \quad (10)$$

In a "small" neighborhood around the nominal steady-state, the process behavior can be linearized leading to the following expressions for ξ and φ:

$$\xi = \left[(KG_x)^{-1}(KG_x^d)\right] ./ \left[G^{-1}G^d\right] \quad (11)$$

$$\varphi = (KG_x)^{-1} ./ G^{-1} \,, \quad (12)$$

in which $./$ means element-by-element division, and G_x, G_x^d, G, G^d represent the gain matrices of the blocks shown in Fig. 1. It is clear from the definition that a desirable property of an estimator K is that $\xi_{i,j} \approx 1$ and $\varphi_{i,j} \approx 1$. Moreover, the steady-state offset $e_{\mathrm{CL}} = r - y$ can be expressed as (Pannocchia and Brambilla, 2002):

$$e_{\mathrm{CL}} = \epsilon_d d + \epsilon_r r \,, \quad (13)$$

in which $\epsilon_r = I - G\left(KG_x\right)^{-1}$ and $\epsilon_d = G\left(KG_x\right)^{-1} KG_x^d - G^d$. It is important to notice that these consistency matrices do not depend on the type of controller used (decentralized or multivariable) as long as the system is square and integral action is used.

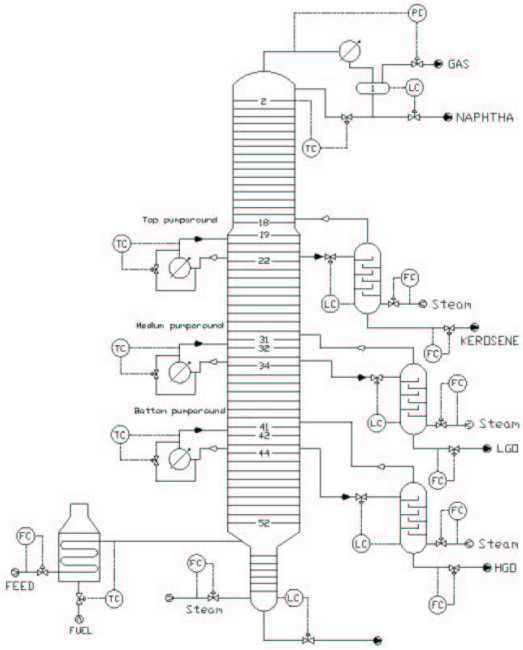

Fig. 2. Crude distillation unit layout with basic control loops

3. PROCESS DESCRIPTION

The crude distillation unit (CDU), which represents the first stage of separation of the crude oil, has the purpose of fractionating the crude oil into a number of products (4-5) with defined boiling temperature ranges. The most common CDU process scheme shows two separation stages: the first (Pre-flash unit) is a partial vaporization of lighter components present in the crude oil, and the second one (Main Fractionator unit) is the separation into products of the components vaporized after the furnace. This unit shows the presence of pumparounds for internal vapor flow reduction and heat recovery, and side strippers that increase the complexity of the unit. The process examined is depicted in Fig. 2, in which only the basic control loops are shown, and it has been simulated by means of the rigorous steady-state simulator Aspen Plus 10.2®. The crude oil, after pre-heating, undertakes a flash (pressure reduction to 4 atm) to remove the lightest components, thus reducing the load of the furnace. Then it is heated in the furnace up to 355 ℃ and, after a further pressure reduction, it enters the column almost at the bottom (this section of the column is known as "flash zone"). The column top product partly condensed constitutes the Naphtha, while several side-stream products as kerosene, light gas oil (LGO) and heavy gas oil (HGO) are drawn off from the column. Each side stream enters a stripper in which usually steam is used to remove the lighter components. From the bottom of the column a stream with heavy components defined as "atmospheric residue" is obtained, which usually undertakes a vacuum distillation. Several liquid streams are taken from the column, subcooled (usually with the fresh feed prior to entering the heat exchanger) and returned to the column a few trays up to condensate part of the vapor going up.

These external cooling systems called “pumparounds” are useful because, reducing the internal vapor flow, they maintain a uniform load of the column by recovering heat.

The product quality is usually defined in terms of boiling range, for example in terms of ASTM D86 95%, which roughly represents the temperature at which 95% of a product is evaporated. Some products as Kerosene and LGO have to meet quality also in terms of “Freezing point” and “Cloud point” (cold properties) which are related to the boiling range, but also to the type of crude processed. In the present work only ASTM D86 95% has been considered as product quality (for simplicity denoted with T95). The setpoint value for T95 of each product is as follows: 173℃ for naphtha, 236℃ for kerosene, 345℃ for LGO and 394℃ for HGO. The top temperature setpoint and side product flow-rate setpoints are the manipulated variables used to achieve these product quality targets. A complete description of all column parameters is available in (Pastore, 2002) and not presented here for the sake of space.

4. ESTIMATOR DESIGN

In this section several estimators for T95 of the four products are built by using the PLS regression with different inputs as auxiliary (measured) variables. As it will be shown, the input selection is the key step of an effective estimator design particularly in terms of closed-loop consistency. It is important to notice that an estimator is designed for each product T95 independently, and this implies that each product property is estimated by means of different inputs. In fact, the product properties are not strictly correlated and a unique “centralized” estimator may lead, in general, to a more interacting multivariable control system and in some cases to infeasibilities.

The training set consists of 152 simulation runs in which the manipulated variables and several disturbances are varied (positive and negative steps) one by one. Moreover, 40 runs correspond to varying one manipulated variable with the other product quality loops closed. In fact, this training set has led to the choice of inputs that guarantee better estimator performance both in terms of accuracy and consistency (Pastore, 2002). It is important to remark that the last set of runs could be difficult to be done on the actual plant, because on-line analyzers for such properties are usually not available. However, rigorous simulators can be used to build a training set that includes closed-loop runs (as well as open-loop ones), and this allows one to choose the most appropriate input locations. Then, the actual estimator coefficients are calculated through a PLS regression on real plant data.

4.1 *Input selection*

For each product quality estimator several inputs have been considered, which consist of a number of tray temperatures, as well as other additional inputs as the operating pressure. The first estimator considered, referred to as E0, uses for each product quality the temperature of the tray where the product is drawn off from the column and fed to the corresponding stripper. Notice that this estimator uses inputs that are always available on a CDU.

Then, for each product quality, an “optimal” location of the temperature measurements is found by using the method proposed by Mejdell and Skogestad (1991, sec. 5.6), which is based on the PLS regression on “all” tray temperatures. It is worth noticing that the column sections included between the draw tray and pumparound return are not considered in this search because the function of those trays is mainly to exchange heat between the two phases by condensing vapor. In fact, the pumparounds present in those section (see Fig. 2) cause intense upsets (due to the condensation of the upcoming vapor) that render the trays in those sections far away from the equilibrium, thus making the temperature measurement not reliable to estimate the product properties. Thus, for each product quality a PLS regression is carried out using all the “potential” temperatures with a number of latent variables chosen by means of the explained variance as discussed in Sec. 2.1. Then, the trays are ranked in descending order of the absolute value of the corresponding PLS estimator coefficient in (6) (for the mean centered and covariance scaled data), and this corresponds to ranking the tray temperatures in order of correlation importance. In fact, since the tray temperatures are centered and scaled with respect to their covariance, a larger estimator coefficient indicates a temperature more correlated to the product quality property.

A large number of estimators have been examined (Pastore, 2002), and the following ones are shown and compared with E0.

- E1, estimator that uses the first three most correlated temperatures.
- E2, estimator that uses the first two most correlated temperatures and the top pressure.
- E3, estimator that uses the first three most correlated temperatures, the top pressure and the mean molar liquid-to-vapor ratio of the section below the product side-stream extraction.

Regarding the pressure the actual input used is the logarithm of the top pressure, and this nonlinear transformation is chosen assuming a relationship between boiling temperature and pressure as for the Antoine’s law. The mean molar liquid-to-vapor ratio, which is computable with a higher or lower accuracy depending on the process scheme of the column (e.g. the presence of unmeasured external flows entering the column) and on the available measurements (e.g. missing temperature of subcooled reflux), is considered as input to improve the estimator consistency, as shown in the next paragraph.

Table 1. Naphtha T95: estimator comparison

ID	Inputs	EV
E0	T_2	82.3
E1	T_2, T_3, T_{23}	92.3
E2	T_2, T_3, p	96.6
E3	T_2, T_3, T_{23} $p, L/V$	97.2

Table 2. LGO T95: estimator comparison

ID	Inputs	EV
E0	T_{34}	49.9
E1	T_{35}, T_{36}, T_{S10}	97.4
E2	T_{35}, T_{36}, p	98.2
E3	T_{35}, T_{36}, T_{S10} $p, L/V$	99.1

4.2 *Accuracy and consistency evaluation*

The four candidate estimators (i.e. E0, E1, E2 and E3) are first evaluated in terms of accuracy in fitting the training data. The inputs used by each estimator of T95 for naphtha and LGO and the corresponding explained variance are reported in Tables 1 and 2, respectively (the corresponding estimators for kerosene and HGO T95 are not shown for space limitations). Moreover, comparisons of E0 and E2 in the training data fitting of T95 for naphtha and LGO are reported in Fig. 3 and 4, respectively. From these results it is

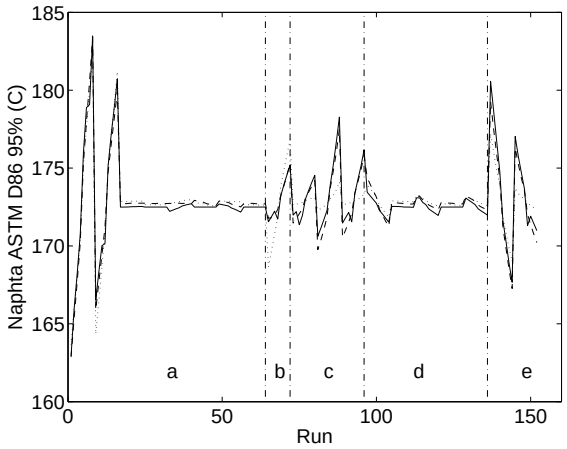

Fig. 3. Naphtha T95: training data fitting (– observ., ··· E0 estim., - - E2 estim.). Data groups: a, external flow changes; b, pressure changes; c, internal flow changes; d, stripper vapor changes; e, feed changes.

clear that an appropriate input selection can improve the estimator accuracy significantly, in particular for changes in column pressure and in internal flows (due to change of furnace temperature and pumparound duties).

Next, the four estimators are compared in terms of consistency for the rejection of several disturbances. A number of disturbances have been considered (Pastore, 2002) and results are presented for variations of the feed flow rate (d_F), of the bottom (d_{BPA})

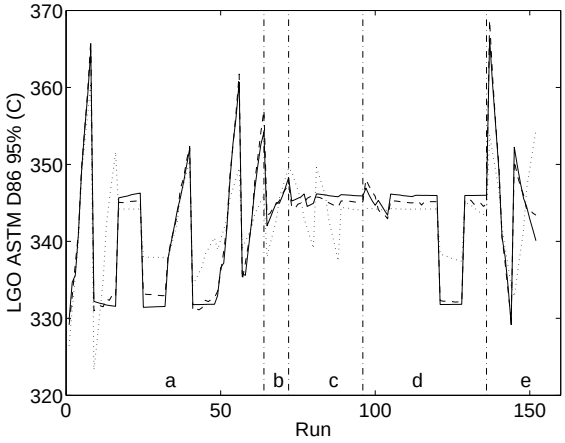

Fig. 4. LGO T95: training data fitting (see Fig. 3 for legend)

and top (d_{TPA}) pumparound duty, of the column pressure (d_P) and of the furnace outlet temperature (d_T). The disturbance consistency parameters for each estimator are shown in Tables 3-6, in which u_1 is the top temperature, u_2 is the kerosene flow rate, u_3 is the LGO flow rate, and u_4 is the HGO flow rate. These

Table 3. Disturbance consistency matrix ξ for E0

	d_F	d_{BPA}	d_{TPA}	d_P	d_T
u_1	0.52	-0.14	-1.10	2.19	-0.24
u_2	1.77	-0.24	-1.27	0.44	0.61
u_3	-4.16	7.15	0.56	3.09	32.18
u_4	19.25	186.16	1.14	3.33	21.44

Table 4. Disturbance consistency matrix ξ for E1

	d_F	d_{BPA}	d_{TPA}	d_P	d_T
u_1	3.35	9.76	-0.77	4.97	14.83
u_2	11.99	-102.20	2.42	4.95	247.65
u_3	55.36	-58.10	14.00	-17.54	-260.83
u_4	-254.66	-2622.21	56.87	-37.88	-373.32

Table 5. Disturbance consistency matrix ξ for E2

	d_F	d_{BPA}	d_{TPA}	d_P	d_T
u_1	0.95	16.97	4.16	5.49	-1.76
u_2	0.98	15.68	0.14	-0.7	-1.54
u_3	0.89	2.56	-1.77	0.92	0.24
u_4	1.05	-2.49	-4.36	0.88	0.59

Table 6. Disturbance consistency matrix ξ for E3

	d_F	d_{BPA}	d_{TPA}	d_P	d_T
u_1	0.98	0.57	1.19	1.03	0.86
u_2	0.85	0.18	1.40	1.01	-1.21
u_3	1.00	0.60	-0.31	0.89	1.4
u_4	1.48	1.80	-0.73	1.4	2.05

results show that E0 is not consistent for almost all disturbances and also that E1 is not very consistent,

even though the accuracy results previously shown suggested that E1 was a well designed estimator. Notice that in Tables 3 and 4 there are several negative parameters $\xi_{i,j}$ that indicate a manipulated variable change of opposite sign than the one actually required to remove offset. The most consistent estimator is E3 for which the parameters $\xi_{i,j}$ are quite close to 1 for almost all the disturbances. The estimator consistency parameters are also evaluated for setpoint changes, and results are shown in Tables 7-10. Notice that the upper part of the consistency matrix is not shown because the 4×4 product quality control system is nearly lower triangular. These results show that E0 and E1

Table 7. Setpoint change consistency matrix φ for E0

	r_1	r_2	r_3	r_4
u_1	0.69	-	-	-
u_2	0.55	0.60	-	-
u_3	-1.42	0.11	0.02	-
u_4	-0.67	-0.7	0.01	0.03

Table 8. Setpoint change consistency matrix φ for E1

	r_1	r_2	r_3	r_4
u_1	1.19	-	-	-
u_2	1.14	4.12	-	-
u_3	15.83	8.07	-11.95	-
u_4	1.30	1.55	1.21	2.97

Table 9. Setpoint change consistency matrix φ for E2

	r_1	r_2	r_3	r_4
u_1	1.16	-	-	-
u_2	1.67	2.10	-	-
u_3	1.86	1.14	2.15	-
u_4	5.677	6.64	5.19	12.22

Table 10. Setpoint change consistency matrix φ for E3

	r_1	r_2	r_3	r_4
u_1	1.00	-	-	-
u_2	1.05	1.27	-	-
u_3	1.30	0.94	1.44	-
u_4	1.12	1.34	1.07	1.63

are not very consistent even for setpoint changes and that E3 is very consistent for setpoint changes in any of the controlled variables.

5. CONCLUSIONS

The design of product quality estimators for refinery main fractionators has been considered, and the PLS regression technique has been used to choose the most appropriate auxiliary measurements. A crude distillation unit was chosen as case study, and several linear static estimators have been designed and compared both in terms of accuracy and consistency for disturbance rejection and/or setpoint changes. An estimator is consistent (Pannocchia and Brambilla, 2002) if it guarantees a low closed-loop offset when inserted in an inferential control scheme, and this property is not necessarily related to the estimator accuracy in fitting the data. It has been shown that the simple use of the temperatures always available on a CDU (i.e. the temperatures of the trays where the side products are drawn) does not lead to a well designed estimator particularly in terms of consistency. The PLS regression has been used to select more appropriate temperature measurement locations but additional measurements, as the operating pressure and the liquid-to-vapor molar ratio, were used to improve the estimator consistency significantly.

6. REFERENCES

de Jong, S. (1993). An alternative approach to partial least squares regression. *Chemometrics and Intelligent Laboratory Systems* **18**, 251–263.

Joseph, B. and C. B. Brosilow (1978). Inferential control of processes. *AIChE J.* **24**, 485–509.

Kano, M., K. Miyazaki, S. Hasebe and I. Hoshimoto (2000). Inferential control system of distillation compositions using dynamic partial least squares regression. *J. Proc. Cont.* **10**, 157–166.

Kresta, J. V., T. E. Marlin and J. F. MacGregor (1994). Development of inferential process models using PLS. *Comput. Chem. Eng.* **18**, 597–611.

Mejdell, T. and S. Skogestad (1991). Estimation of distillation composition from multiple temperature measurements using partial-least squares regression. *Ind. Eng. Chem. Res.* **30**, 2543–2555.

Morari, M. and G. Stephanopoulos (1980). Optimal selection of secondary measurements with the framework of state estimation in the presence of persistent unknown disturbances. *AIChE J.* **26**, 247–258.

Pannocchia, G. and A. Brambilla (2002). Consistency of property estimators in multicomponent distillation control. Accepted for publication in *Ind. Eng. Chem. Res.*

Pastore, D. (2002). Estimator design for the product quality of complex columns (in italian). MS Thesis in Chemical Engineering, University of Pisa.

Wold, S., J. Trygg, A. Berglund and H. Antti (2001*a*). Some recent developments in PLS modeling. *Chemometrics and Int. Lab. Systems* **58**, 131–150.

Wold, S., M. Sjöström and L. Eriksson (2001*b*). PLS-regression: a basic tool of chemometrics. *Chemometrics and Int. Lab. Systems* **58**, 109–130.

Yu, C.-C. and W. L. Luyben (1987). Control of multicomponent distillation columns using rigorous composition estimators. In: *Distillation and Adsorption*. IChemE Symposium Series. The Institution of Chemical Engineers. Brighton, UK. pp. A29–A69.

ACTUATOR SELECTION BASED UPON MODEL INSIGHTS FOR AN ENERGY INTEGRATED DISTILLATION COLUMN

Hong Wen Li, Rafiqul Gani, Sten Bay Jørgensen

CAPEC, Department of Chemical Engineering
Technical University of Denmark
Lyngby, Denmark

A method for development of actuator structures based upon model insight is presented. The method contains three steps. First dynamic degrees of freedom are handled using suitable level actuators and control loops. Second the feasible operating region is developed and third static control structures are proposed and screened. The advantage of the three-layered strategy is that the second and third layers can be dealt with early during process development while the first layer may assure perfect control initially. Later during process design where dynamic process information is available the dynamic loops of the first layer may be designed and subsequently high level control can be designed to fit appropriate control objective for plant.

Keyword: Control, design, integrated, distillation column

1. INTRODUCTION

Chemical process plant design and operation based on combining mathematical models with computer science have the potential to significantly increase the efficiency of manufacturing systems by integrating the design with the planning of operation. Because a chemical plant may have thousands of measurements and control loops, which can be divided into several layers:

1) scheduling (weeks)
2) site-wide optimization(day)
3) local optimization/predictive control (minutes)
4) regulatory control (second)

This paper considers the local optimization layer which recomputers new set points only once an hour or so, whereas the feedback layer operate continuously. The layers are linked by the controlled variables and the selection of the control configuration, whereby the set points are computed by the upper layer and implemented by the lower layer.

Therefore it is essential to investigate operability of such complex processes at the design stage in order to enable suitable design modifications before it is too late. The systematic computer aided pre-solution analysis of process models for integrated design and control presented earlier by Russel et al. (2002) is further investigated in this paper for an energy integrated distillation pilot plant. This paper investigates aspects of design and control of the integrated distillation column with the model analysis method and validates the results through simulation and operational analysis of the energy integrated distillation column. First the steady state control configuration is obtained for column; subsequently. The dynamic behaviour of the heat integrated distillation column is discussed.

2. PROCESS DESCRIPTION

The heat integrated distillation pilot plant considered in this paper is shown in Figure 1. It contains two main sections, namely a distillation column section and a heat pump section. The heat pump section is physically connected to the distillation column through the condenser at the top and the reboiler at the bottom of the column. The heat pump consists of four heat exchangers, two compressors, one expansion valve, a large tank, α_{CV8} and α_{CV9} are the control valves. While the refrigerant circulates within the heat pump it changes phase, and through

absorbing heat of vaporization at low pressure and releasing it again at high pressure it carries heat from the column condenser to the column reboiler. A more detailed description of this pilot plant is given by Eden et al. (2000). The process model analysis of these two sections is discussed individually.

3. PROCESS MODEL ANALYSIS

Model analysis first determines the available degrees of freedom for design and for control, which then identifies the "common" variables used in design as well as control. The analysis subsequently identifies the important constitutive equations, their dependent process variables and the corresponding derivative information with respect to the identified "common" variables. This analysis employs the mass and energy balance equations and the constitutive equations to generate information related to process sensitivity, process feasibility, and design constraints. The model analysis is decomposed into two parts: first the analysis is carried out for the distillation column and thereafter, the heat pump system.

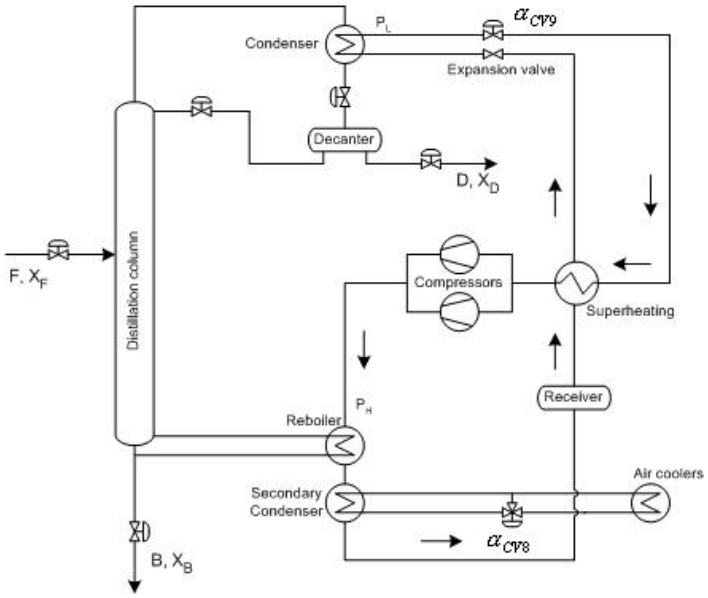

Figure 1: Flow sheet of the heat-integrated distillation column

3.1 The Process Model Analysis for the Distillation Column

Five degrees of freedom are related to five design and control variables. A design problem could be to determine the optimal values of the design variables so that some process variables attain their desired values. A control problem could be to maintain the same process variables at their desired values by manipulating the same design variables when there is a disturbance. When the design and control problems involve the same set of variables, they may be integrated and solved simultaneously, once an integrated problem has been formulated.

From a control point of view, for dual composition control of the distillation column, both the top product purity and the bottom product purity need to be controlled. The hold ups of the condenser and boiler are needed to be controlled to stabilize the system. For example the optimisation variable or design variable D (distillate flow rate) is used to control top composition x_D and vapour flow rate at the bottom V_B is used to control bottom purity x_B, where vapour flow rate is manipulated by heat duty of the reboiler Q_B. The column pressure is controlled by heat removed from the condenser Q_C. The hold ups of the condenser M_D, is controlled by reflux flow rate L_0 and the hold up of reboiler M_B is controlled by bottom product B. Hence for control purpose, the design optimisation variables, Q_B, Q_C, D, L_0, B may be chosen as the manipulated variables. This illustrates the relationship between design and control issue for a conventional distillation column.

From a design point of view, the five design variables are selected first. The product rate D and B need to be specified to meet the external mass balance and the market needs. Vapour flow rate V, the condenser heat duty Q_C and reflux flow rate L_0 are needed in the column to fulfil the separation process.

3.2 The Model Analysis for the Energy Integrated Distillation Column

From the model analysis, two degrees of freedom are obtained for the heat pump section. Here high pressure on heat pump section P_H and low pressure P_L are chosen as controlled variables. Two actuators are valves α_{CV8} and α_{CV9}.

4. OPERATION WINDOW FOR THE ENERGY INTEGRATED DISTILLATION

The appropriate variables that can be controlled through the identified "common" design/actuator variables can be identified through an investigation of the operation window. In the case of this heat integrated column with sieve trays operated primarily in the spraying regime, the limits forming the operating region are the flooding limit, weeping limits, maximum column pressure, maximum heat pump high pressure, maximum heat pump low pressure, maximum cooling power of the heat pump system, maximum pumping capacity. Inside this region is the operation window, within which the operation point must be located to ensure the separation process (as illustrated through Figure 3). The empirical correlations for flooding and liquid weeping are described below and the limits related to the high and low pressures of the compressor system are determined through simulation.

4.1 Flooding and Liquid Weeping Curves

The following derivations are based on empirical correlations estimated by several authors and collected by Zuiderweg (1982) on his review paper on the state of the art for sieve trays. Let L_0 and V be the volumetric flow rates of reflux and boil-up in m^3/s, and let ρ_l and ρ_g be the liquid and gas densities in kg/m^3. The weeping limit in terms of the minimal vapour flow rate is then found by the following empirical correlations:

$$V_{\min} = CF_w . A_t \sqrt{\frac{\rho_g}{\rho_l}} \qquad (1)$$

Where: CF_{max} is the tray capacity factor on bubbling area, m/sec
A_t is the tray area, m^2
This correlation is plotted as the weeping limit, i.e. Curve 1 in Figure 3
The flooding limit in terms of the maximal vapour flow rate is used as the flowing correlation:

$$V_{\max} = CF_{\max} . A_t \sqrt{\frac{\rho_g}{\rho_l}} \qquad (2)$$

Where CF_{max} is the capacity factor at start of flooding, m/sec. This correlation is plotted as the flooding limit, i.e. Curve 3 in Figure 3

4.2 Maximum and Minimum P_L

The limits of the operation region imposed by the heat pump are obtained by simulation in total reflux mode. Curve 2 in Figure 3 is mapped by switching on a controller to maintain heat pump low pressure P_L at its maximum, i.e., 600kPa and then gradually decrease high pressure P_H until intersection with the weeping limit. Going along this trajectory the number of active cylinders reduced as appropriate such that the pressure drop through α_{CV9} has a reasonable level (50-200kPa). If the pressure drop exceeds these limits retuning of the low pressure controller is necessary due to the nonlinear valve characteristic. Curve 4 in Figure 3 is mapped by keeping α_{CV9} open and all cylinders active, and then gradually decrease high pressure P_H. This way the low pressure is at all time kept as low as possible, decreasing as the high pressure is reduced. The lower limit represents the lowest possible column pressure, and it crosses the weeping limit at a point, which thus is the point of lowest possible column pressure and boil-up rate at which the column can be operated.

5. THE STATIC ACTUATOR CONFIGURATION OF THE INTEGRATED DISTILLATIO COLUMN

From the analysis of process model for the distillation column in Section 3 five degrees of freedom are obtained, which related to five design and control variables. The vapour flow and column pressure are controlled by manipulated the heat duty of reboiler Q_B and condenser Q_C. But For integrated distillation column Q_B and Q_C are not the manipulated variables, which are controlled by P_H and P_L on the heat pump section. In order to get a suitable control configuration the gain of P_H and P_L to the column pressure and vapour flow rate are investigated through simulation. The results are shown in Figure 2 from which one can see that P_H has positive gain to column pressure and vapour flow rate and P_L has positive gain to column pressure but negative gain to vapour flow rate. From this understanding it is seen that in order to increase the column pressure at constant boil-up rate one must increase both actuators, while if the boil-up rate is to be increased at constant column pressure (either P_B or P_C) one must increase P_H and reduce P_L. So it is clear that specifying the two heat pump pressures P_H and P_L is equivalent to specifying boil-up flow rate and column pressure and hence it should be possible to configure a control system manipulating the set points to the high and low pressure Through the analysis of the column the actuator structures above, it appears that P_H+P_L (on the heat pump side) is suitable to the control column pressure while P_H-P_L (on the heat pump side) may be used to control the vapour flow rate. With these control actuator configuration, the column pressure and vapour flow rate control loops are decoupled. This also means that the actuator (design) variables on the distillation column side are determined through the "control"

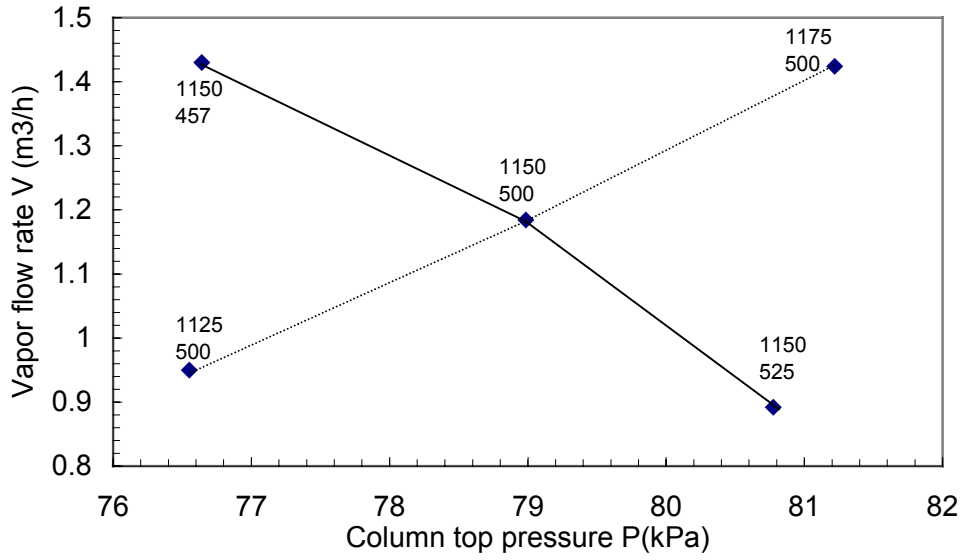

Figure 2: The gain for positive and negative changes in the heat pump pressures. Steps $\pm 25kPa$ in high and low heat pump pressures (on simulation plot: P_H over P_L in kPa)

variables on the heat pump side. Rigorous simulations have been performed to confirm the actuators configuration with the dynamic model of Koggerbøl (1995). The simulation results are plotted in Figure 3, where the curve A in Figure 3 is at constant P_H+P_L, while P_H-P_L change. From curve A one can see that column pressure is nearly constant for constant P_H+P_L for many different P_H-P_L. From curve B one can see that the vapour flow rate is nearly the same at constant P_H-P_L in spite of different P_H+P_L. This confirms the design and control issues stated above that one could control the vapour flow rate in the integrated distillation column by manipulating the pressure difference between the high pressure and the low pressure of the heat pump side and the column pressure by manipulating the sum of the two heat pump pressures. This control structure is implemented to the column. A tool for real-time multivariable identification and control for the integrated distillation column is named Multi Input and MultI Output Selftuning Controller (MIMOSC). The basic structure of the controller is used for controlling the column pressure and the boil-up vapour flow rate. The steady state control structure is obtained for the integrated distillation column. Next paragraph a dynamic control structure is discussed .

6. CONTROL STRUCTURE FOR DYNAMIC INTEGRATED DISTILLATION COLUMN

6.1 Dynamic Control Structure for Column Section

For the distillation column, the overall control for the column section has five outputs X_D, X_B, M_D, M_B and P. Compared to the static control problem, two more holdup variables, i.e., M_D and M_B, are introduced. Suppose that the column pressure and the reboiler vapour flow have the same control configurations as the steady state. For such kind of "standard" control problem, the most widely accepted control structures are "LV-configuration" or "DV-configuration.

The issue of this kind of control configuration has been investigated using frequency dependent formulations of measures such as the condition number, the Relative Gain Array by Bristol (1966) and the Relative Disturbance Gain by Stanley et al (1985). This paper will focus on discussing the dynamic control structure on the heat pump section and how each dynamic control structure affects the stability of the integrated distillation column.

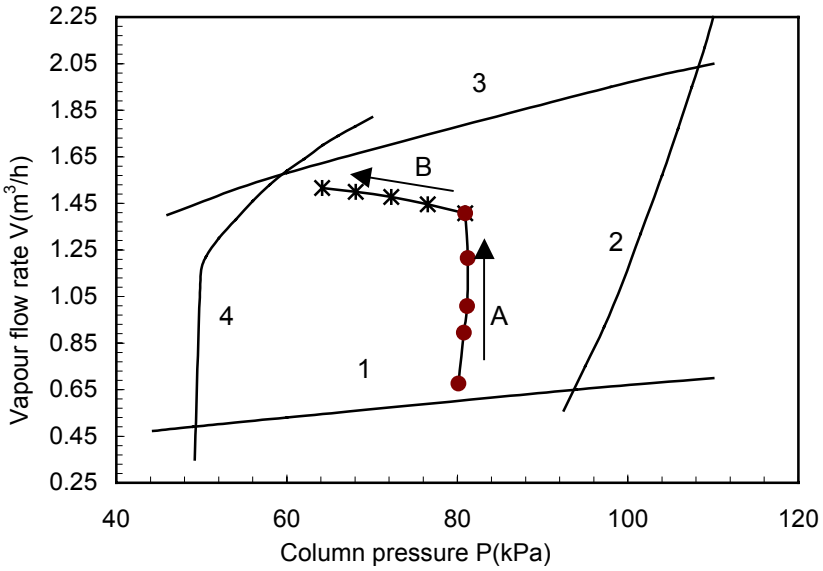

Figure 3: A curve: P_H+P_L at constant, P_H-P_L change; B curve: P_H-P_L at constant, P_H+P_L change

6.2 Control Structure on the Heat Pump Section

As discussed above, P_H+P_L and P_H-P_L are used to control column pressure and vapor flow rate. In turn, P_H and P_L are controlled by manipulating two actuators α_{CV8} and α_{CV9}. The pair of these two process variables and two control valves play a very important part in terms of stabilization of the integrated distillation column. First let us discuss how disturbance affects the heat pump high pressure P_H and low pressure P_L so as to decide the pair problems. Consider, for example, the plant at steady state with only liquid level controllers for the reboiler and the condenser has been implemented. If suddenly the energy balance is disturbed by a small amount δH, for instance due to a disturbance in the feed preheater in the feed composition, or perhaps in the temperature of the cooling medium in the secondary condenser, then the changed heat input starts to accumulate in the plant. If the disturbance reduces the cooling rate this will immediately affect the high pressure P_H such that P_H begins to increase. Thereby the compression work is continuously increased, but also the cooling rate will gradually increase as the temperature gradient in secondary condenser and in the air coolers will increase with P_H. The increase in the high pressure affects boil-up rate, and as a result of this, the column pressure and the heat pump low pressure P_L simultaneously increase. Assuming that the enthalpy of the feed remains constant after the disturbance, the behavior of the entire plant becomes unstable if the compressor work increases faster than the sum of all the outgoing heat flows. For this integrated distillation column the compressor work does indeed increase faster than the sum of all the outgoing heat flows within part of the operating region. Therefore a small disturbance in the overall energy balance can initiate a drift of the plant towards increasing or decreasing pressures depending on the sign of the disturbance. To reject disturbance so as to stabilize the system, high pressure P_H and low pressure P_L need to be controlled by manipulating suitable actuators. In theory either the low pressures or the high pressure could be paired with α_{CV8} and thereby stabilizing the system. However, the gain from α_{CV8} to the low pressures is relatively small (Koggerbøl, 1995) so if α_{CV8} is to be used for stabilization it should be preferably be paired with the measurement of P_H.

The valve α_{CV9} does not directly affect the energy balance but it can be used to stabilize the plant if it is paired with a suitable measurement. Suppose that P_L is stabilized by manipulating the valve α_{CV9} then a disturbance, which tends to increase P_L, will be neutralized by the valve opening being increased by the controller. This way P_L is maintained at setpoint.
The main result of the discussion above is that high pressure P_H should be controlled and that the cooling valve α_{CV8} is preferred as actuator for this purpose. So, in conclusion, a control loop manipulating α_{CV8} based on a measurement of the high pressure P_H is suggested to stabilize the plant. The low pressure P_L is controlled by control valve α_{CV9} to stabilize the system. In the reboiler the saturation pressure P_H is a sufficient measure of the condition on the freon side for heat transport into the column, This condition is now going to be controlled using α_{CV8}. In the condenser, which is the other contact point between the heat pump and the column, the saturation pressure P_L is a sufficient measure of the condition on the freon side for heat transport from the column. So this control structures, i.e., valve α_{CV9} control low pressure and valve α_{CV8} control high pressure, can reject the disturbance and stable the system.

7. CONCLUSION

With a systematic computer aided analysis of the process model inspired by Boris et al, the control and design problems for an energy integrated distillation

column are carried out. The relationships between design and control problems are discussed through analysis of the process model to result in a more suitable control actuator configuration for the integrated distillation column. Rigorous simulation results verify this analysis.

A method for development of actuator structures based upon model insight is presented. This paper addresses how to select and combine actuators in order to achieve nearly independent actuator actions. Thereby the interactions between basic control loops in the integrated distillation column are significantly reduced which is the basis for optimising control. Thereby this paper demonstrates that integration of design and control insights can lead to much more than was claimed by Russel et al. (2002).

8. REFERENCES

Bristol, E.H., (1966), On a New Measure of Interactions for Multivariable Process Control. IEEE Trans. Automat. Control, AC-11, 133-134.

Eden, M. R., Køggersbøl , A., Hallager, L. and Jørgensen , S. B. (2000), Dynamics and control during startup of heat integrated distillation column Computer and Chemical Engineering, 24 1091-1097.

Koggersbøl, A.,(1995), Distillation Column Dynamics, Operability and Control. Ph. D Thesis, Technical University of Denmark, Denmark.

Russel , B. M., Henriksen , J. P., Jørgensen , S. B. and Gani, R. (2002). Integration of design and control through model analysis, Computers and Chemical Engineering, 26(2), 213-216.

Stanley, G., Marino-Galarraga, M. and Avoy, Mc. (1985). Shortcut Operability Analysis. The Relative Disturbance Gain. Industrial Engineering & Chemical Process Design Development 24(4), 1181-1188.

Zuiderweg, F.J. (1982). Sieve Trays: A view on the State of the Art; Chemical Engineering Science. 37(10). 1441-1464.

STUDY ON THE SOFT-SENSOR AND CONTROL SCHEME FOR AN INDUSTRIAL AZEOTROPIC DISTILLATION COLUMN*

Shi Zhang, Cuimei Bo, Jun Li, Changyin Sun, Yanru Wang

College of Automation, Nanjing University of Technology, Nanjing 210009, China
E-mail: zhangshi@njut.edu.cn

Abstract: In this paper, control problems of an industrial Azeotropic distillation column were discussed and improved. At first, the soft-sensor of water content in the bottom of the column was built based on on-the-spot data collected by distributed control system (for short, DCS), through applying soft-sensor technology of regression, and a self-correcting module was also designed. The functions of estimation, display and correction about water content were realized on the DCS. At the same time, according to the actual quality control targets, an inferential control scheme based on soft-sensor was designed, in which the on-line estimating values of soft-instrument were used. The close-loop control of the product quality was realized in the scheme. As a result of increasing of Boolean calculation with constrained condition in the inferential control arithmetic, the reliability and practicability of the control system is strengthened. Application of the control system to the column showed that the control system can resolve effectively the problems that the product quality cannot be measured on-line and be close-loop controlled directly, and has realized the bounder control of water content in the bottom of the column.

Keywords: azeotropic distillation, regression and analysis, soft sensor, inferential control

1. INTRODUCTION

Distillation is the most important unit operation for separation processes commonly adopted in petroleum refinery and chemical industry. Because of the difficult factors, such as nonlinear, multi-variables, hard to measure quality factors online, the automatic control problem for distillation process has always been one of the hot subjects of automation researches. Many articles on distillation column controlling have been issued (Kumar, *et al*., 1999; Monroy *et al*., 1999). From the industrial facts, there exist the distillation columns with control problem (Ming Rao, *et a*l., 2002), which are seldom able to guarantee the products' purity mostly accounting for their overly simple control systems (I-Lung Chien, *et al*., 2000). Therefore, the excess purification is usually adopted in practice operation, which increased energy consumptions as well as decreased the product yield.

Recently, DCS is often introduced to control industrial equipment, especially in larger petrol-chemical plant. A contradict phenomenon arose in those petrol-chemical enterprises. In this paper, An advance control system based on DCS was proposed and designed, which has mainly relies on the present functions of DCS and improved the control of an industry distillation column.

2. PROCESS INTRODUCTION

The main subject of this article is focused on the workshop of butadiene-producing equipment, which existed almost all of the petrochemical enterprise.

* The researches of paper are sponsored by the corporation, contract No: 01JSNJYZ101015

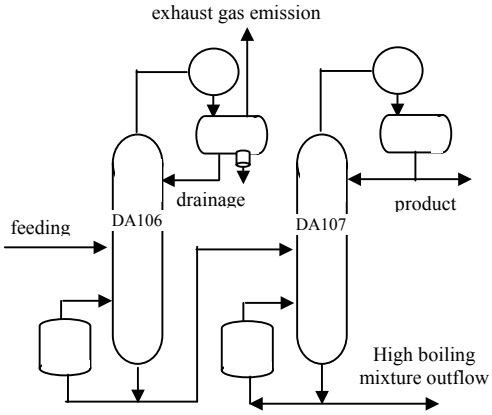

Fig.1 the flow sheet of butadiene distillation workshop section

Butadiene is the major monomer and raw material for producing styrene butadiene rubber, cis-1.4-polybutadiene rubber, nitrile rubber, ABS rosin and nylon. The distillation workshop section of butadiene produce equipments includes two distillation columns, Column DA106 and Column DA107, whose tasks are to remove the high-boiling-point impurities, such as cis-butene-2, butadiene-1, 2, ethyl acetylene and C_5, as well as low-boiling-point impurities such as methyl acetylene and water, and to achieve the final product, butadiene-1, 3. There are some control problems in the two distillation columns. Column DA107 is the production column. On the purpose of enhancing the operating and controlling level in the producing procedure, meeting the requirements of social economy, the former conventional control system has been changed into DCS system. Therefore, a set of control scheme need be improved accordingly. The improved scheme of Column DA107 has been reported in (Shi Zhang, *et al.,* 2002). In this paper, the control problem of water content about Column DA106 will be discussed.

The basic producing flow sheet of distillation workshop of butadiene-producing equipments is showed in the Fig.1.
Though most of the impurity has been dropped out from the raw material C_4 in the previous extraction distillation workshop, some impurities whose volatilities are close to butadiene-1,3 still exist. These impurities are to be dropped out in the columns of DA106 and DA107.
Column DA106 is an azeotropic distillation column with the main task of dropping out methyl acetylene, water and other lighter components. Methyl acetylene and other lighter components rise into the top of Column DA106 because of their low boiling point. Then they will be cut out with part of butadiene-1, 3, as the tail-gas into torch. The saturated water in feeding, as the azeotropic matter of butadiene-1, 3, is also taken to the top of the column. It is delaminated with butadiene in the circumfluence jar after condensation, and then is drained out from the bottom of the jar.

Water content in feeding is about 500(mg/kg), but in the products' purity index, the water content should not be over 20(mg/kg). The task of Column DA107

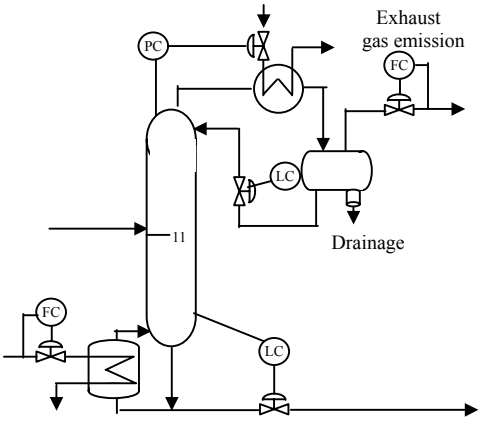

Fig.2 the flow chart with reference point of column DA106

is to take off high-boiling mixture, namely, all the water in the bottom of Column DA106 will be carried into products, besides, through the experience of operators, if the water content is well controlled, the methyl acetylene consistency index is able to be guaranteed. As a result, the water content is a vital controlling target.

The Figure 2 indicates the former controlling scheme of Column DA106. From the figure, it can be seen that this scheme is formed by all simple loops, without any quality-controlling loop. What's more, the current producing load goes far beyond the system's designing ability. Therefore, the former controlling scheme is hardly to fulfil the controlling task. In this case, the operators usually turn to the controlling method of increasing heat supply of the reboiler. The method pledges that the water content keeps not more than 20(mg/kg); however, it increases energy consumption. In addition, the water content in the production is also not stable.

In view of this case, the inferential control based on soft-sensor is designed instead of the former fixed value control system of the reboiler's heat supply, which can realize the direct quality control of water content. The key problem of the work is to solve the soft-sensor of water content.

3. THE SOFT-SENSOR OF WATER CONTENT

In recent years, it is widely reported that the soft-sensor technique has been introduced into the component estimation (Jingshou Yu, Ailun Liu, Kejin Zhang, 2000). Lots soft-sensor instruments in the form of commercial software have been released and utilised in practice production. Nevertheless, these softwares are so expensive that they were rarely introduced by the domestic enterprises. Soft sensor instrument, also soft sensor model, is the nuclear problem of the soft sensor technique. In the several modelling method, artificial neural network and regression analysis methods are often adopted. Because of the condition in factory, regression analysis method was selected to build the soft sensor model.

3.1 Assistant variable Selecting and analysis data setting

In this work, the possible process variables related with water content which can be obtained with soft-sensor instruments are as follows: two temperatures (the reboiler heating temperature T500-25 and the bottom temperature T500-26), three fluxes (the reboiler heating flux F133, the feeding F122, and the circulatory flux F134), one pressure (the bottom pressure P116) and one liquid location (the bottom liquid location L119).

As for the seven variables shown above, T500-25、T500-26、F122、F134、P116 are chose as process assistant variables. With the action of fixed value controlling loop, F133 and L119 are kept stable and remain fixed. And which have little to do with the change of water content, so the both variables are omitted. According to the result of the regressing analysis method, the five parameters above-mentioned are obviously connected with the water content, while F133 and L119 give no effect on water content. Lots of high frequency noises existing in measured value of the flux, which may influence the modelling work, so the measured value of F122 and F134 must be filtered at first, and then to do regression analysis.

Another difficult problem is that there is no practical value of the water content at the bottom of the column DA106, only a test point located at the exit of column DA107 (product jar) for sampling and analysing water content every 8 hours. Consider that the water content in the product will not change a lot from the bottom of Column DA106 to the product jar, it can be supposed reasonably that water content in the product jar is only the express of water content in Column DA106 bottom after a period of delaying-time (τ). At the same time, some analysis values of water content in the column DA106 were added temporarily. And according to comparison of the both curves between these analysis values and those in the product jar, the same conclusion was made, also with the experiences of the operators, the value of τ is confirmed about 1 hour. As a result of the water content at the bottom of Column DA106 can be shown by the analysis value of the water content in the product, the analysis values of water content in the product jar were used as the estimated variable of the soft sensor model.

3.2 Building the soft-sensor model

The abundant on-the-spot data (420 groups), which were collected by distributed control system, were classified as the two parts: the modeling set (300 groups) and the verifying set (120 groups). A soft sensor model is built with regression and analysis technology based on the modeling set (300 points). The regression model can be shown as follows:

$$S_{130}(t) = \sum_{i=0}^{5} a_i \times x_i(t-\tau) \qquad (1)$$

Where:

$S_{130}(t)$: the estimated value of water content at t;

τ: Delaying-time;

$x_i(t-\tau)$ (i = 1, 2, …, 5): 5 assistant variables;

a_i (i = 0,1, 2, …, 5):Regressing-coefficients.

The values are:

a_0	-84.677507
a_1	2.841364
a_2	-0.655388
a_3	-1.731556
a_4	1.582286
a_5	231.365314

The verifying set data are used to verify the model's extrapolative ability. The results of the model's simulation and extrapolation are shown in Fig.3.

In the Fig.3, the abscissa values show sampling numbers. It is obvious that the precision of the proposed model is very high, and the extrapolative ability can also satisfy the control request. Moreover, the model is simple in form and easy to realize in the project.

3.3 On-line correcting the soft-sensor model

Because of the influences from time varying, nonlinear and no integrality of modeling factor established in product process, the soft-sensor model has to be corrected on-line (Jingshou Yu, 2002). The correction work may classify into two types. One is long-time correction, that is, after the distillation process running for a period of time, a new model will be reconstructed and substituted the former model; the other is short-time correction, which is carried out on-line, it means that the short correction is to correct the model with the error between the analysis value every 8 hours and the calculating value of soft-sensor model. What requires our attention is that the time when the analysis data is sent to the control-room delays the sampling time

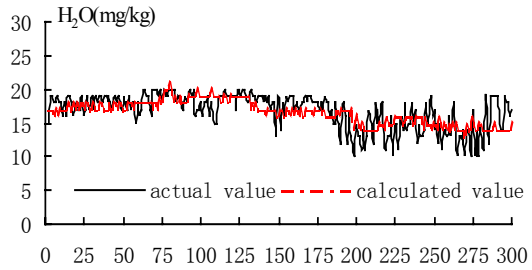

Fig.3(a) Training plot of the regression

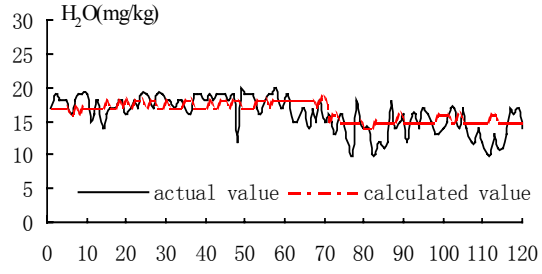

Fig.3(b) Verifying plot of the regression

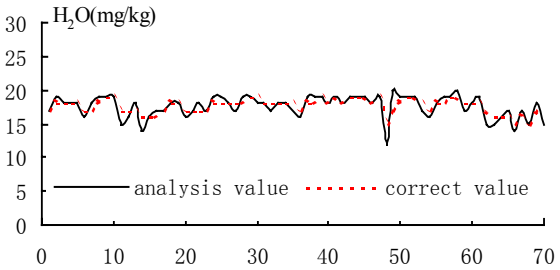

Fig.4 on-line corrected effect of soft-sensor model

about δ time, so the calculating value at the moment of sampling should be kept in order to compare the two groups of data at the same time. Correction formula is as follows:

$$\Delta S_{130}(t) = \alpha \times [S_{\alpha 130}(t-\delta) - S_{130}(t-\delta)] \qquad (2)$$

Where：

$\Delta S_{130}(t)$:The corrected value of the water content at *t;*

α: The corrected coefficient, here is 0.5;

δ: The analysis delay-time;

S_{a130} (*t*- δ): The analysis value of the water content at *t*- δ*;*

S_{130} (*t*- δ): The estimated value of the soft instrument at *t*- δ.

From the Fig.4, on the condition that the extrapolate ability of the soft-sensor mode is not very better (see the Fig.3), only through on-line correcting, the accuracy of the soft-sensor mode has be advanced so that the soft sensor model corrected on-line may be applied to the practice.

4、THE CONTROL SCHEME AND PRACTICAL APPLICATION

As shown above, the prime problem about the control system of column DA106 is that there are not direct or indirect quality control loops. So the operators adjusted the given value in control loop of reboiler heating flux by hand, only basing on sampling analysis data every 8 hours, to control the water content of the column bottom. Under this distillation operation condition, not only the water content in the product jar cannot be ensured availably, but also the energy consumption is increased greatly. Therefore, an inferential control scheme based on soft sensor is designed to substitute the former control loop of the water content in the column bottom.

4.1 Basic control scheme

There is a basic control scheme shown in following Fig.5.
In the figure, the soft-sensor instrument is just the soft-sensor model built above.

In view of the possibility of project realization, the water content controller only adopts PID arithmetic. So, except the soft-sensor model needs to program in Command language, all the control schemes are easily carried out by configuration in DCS.

On the DCS of the column, the control scheme was put in practice, and tried to run for a period of time. It is proved that the scheme is available. Firstly, the control effects of water content is so ideal that the value can be controlled between 18~20(mg/kg). Secondly, the heating of reboiler was decreased than before.

4.2 Constrained control in the control scheme

At the same time, when the work situation changed greatly, this control scheme could not run steadily for a long time. It is reason that along with the great change of the word situation, the great fluctuation of control variable occurred. Therefore, the condition of work might also leave the perfect balance condition.

Through analyzing the technique process, the reason caused this phenomenon was found. When control variables are changed greatly, the rising steam capacity within the column is influenced. In Figure 2, for the circulatory flux is the control variable of liquid level of reflux tank, the large change of the rising steam capacity quickly causes the circulatory flux fluctuates greatly. However, this fluctuation could not be allowed. According to the rule of should

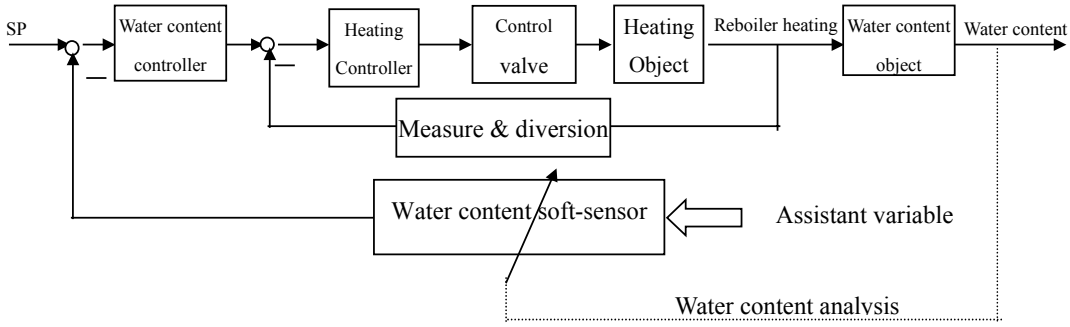

Fig5 water content inferential control system flow chart of DA106 column bottom

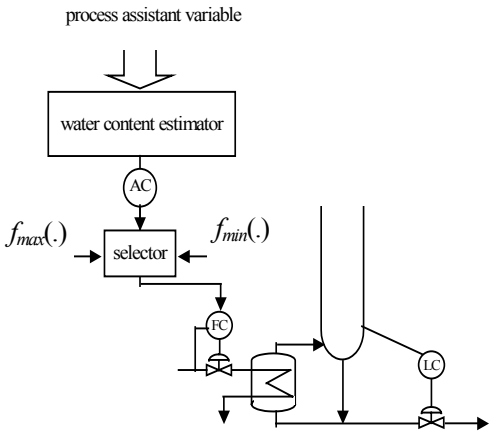

Fig.6 Improved inferential control scheme

control techniques, the circulatory flow in the column be limited between 1.3 to 1.7 times of feeding. For these reasons, a constrained control with the logic module is added to the above inferential control scheme. The inferential control scheme with constrained control is shown in the Fig.6.

The relation between input and output in the selector is:

$$out = \begin{cases} f_{\max}(.) & if \quad out_{AC} \geq f_{\max}(.) \\ out_{AC} & if \quad f_{\min}(.) \leq out_{AC} \leq f_{\max}(.) \\ f_{\min}(.) & if \quad out_{AC} \leq f_{\min}(.) \end{cases} \qquad (3)$$

Where:

out: The output of selector;

out_{AC}: The output of water content's controller;

$f_{max}(.)$: The maximal heating;

$f_{min}(.)$: The minimal heating.

Here $f_{max}(.)$ and $f_{min}(.)$ are decided by following process:

(1) Through analyzing the technique process, the technique parameters are decided which are all related with heating of reboiler, including the feeding F122, the circulatory flow F134, the temperature of heater's input and output T133 and T500-25, the column bottom temperature T500-26 and pressure P116;

(2) The regress relation, f (F122, F134, T133, T500-25, T500-26, P116), was obtained by regression analysis with the field data;

(3) Supposing the circulatory flow is enhanced to 1.7 or 1.3 times separately, then the maximal heating and the minimal heating function $f(.)$ are listed as follow:

$f_{max}(.)= f$ (F122, 1.7×F134, T133, T500-25, T500-26, P116)

$f_{min}(.)= f$ (F122, 1.3×F134, T133, T500-25, T500-26, P116)

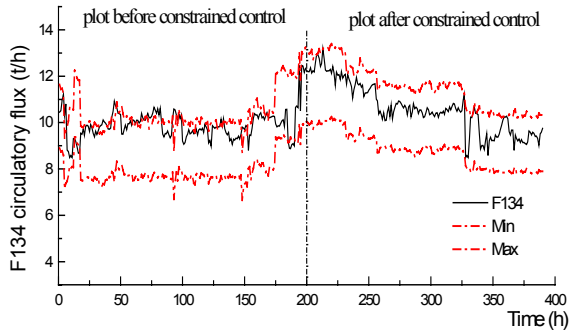

Fig.7 the effect of the comparison of before and after the constrained control

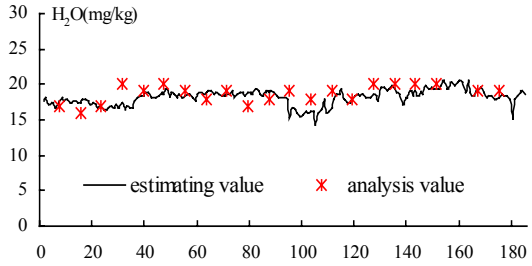

Fig.8 the practical effect of inferential

After the constrained control of the circulatory flow was added to the inferential scheme, the circulatory ratio can be controlled effectively in the rational scope. So the phenomena of the bigger circulatory ratio could be avoided, that is the water content of the column bottom is too lower. The Fig.7 shows the result of the comparison effect that the constrained control has be applied to the worksites.

4.3 The practical application of control scheme

The control scheme has been applied preferably to the column DA106 for half of years. Figure 7 gives the real time control effect. In the Fig.7, it is shown that the fluctuation of water content in the product is on the small side after the control scheme has been applied to the column. It can be controlled within the17~20(mg/kg) scope, which justly meet the control goal that the water content in the product is less than 20(mg/kg). At the same time, the change of the circulatory flow also became relatively steady, and the energy consumption was decreased greatly.

5.CONCLUSIONS

In this paper, aiming at an industrial azeotropic distillation column, an inferential control scheme with constrained control was designed to substitute the former control scheme of column. And the bounder control of water content in the bottom of the column has been realized. Firstly, a soft-sensor model and an inferential control scheme based on the soft sensor model are build and designed. Then, according to the practical running, the constrained control is added to the scheme. As a result of Boolean calculation added to the control arithmetic, the robustness of the control system is strengthened. So the system could be able to adapt preferably great fluctuation of work situations. Through the several months of practical application, it proved that the control system is feasible and available to run steadily for long time.

REFERENCES

I-Lung Chien, Wei-Hung Chen, Tsun-Sheng Chang (2000). Operation and Decoupling Control of a Heterogeneous Azeotropic Distillation Column, Computers & Chemical Engineering, 24(2): 893-899

Jinshou Yu, Ailun Liu, Kejin Zhang (2000). Soft-sensors for the petro-chemical industry, chemistry industry press, Beijing , pp.122, in Chinese

Jinshou Yu (2002). Industry Process Control, China petrochemical industry press, Beijing, pp.270, in Chinese

Ming Rao, Jilu Feng, Jinming Zhou (2002). An Intelligent System for Real-time Monitoring and Fault Predicting, Proceedings of WCICA 2002, p2737~2741, June 10-14, Shanghai

Monroy Loperena, Rosendo, Alvarez Ramirez, Jose (1999). On the steady-state multiplicities for an ethylene glycol reactive distillation column, Industrial & Engineering Chemistry Research, 38(2), 451-455

Shi Zhang, Cuimei Bo, Qingcheng Dai, Jinguo Lin (2002). Inferential Control Scheme and Soft-sensor model of Butadiene Distillation Column, Process Automation Instrumentation, 23(9), 59-61, in Chinese

Shurong Li, Haitao Shi, Feng Li (2002). RBFNN Based Direct Adaptive Control of MIMO Nonlinear System and Its Application to a Distillation Column, Proceedings of WCICA 2002, p2896~2900, June 10-14, Shanghai

Xiaoming Jin, Gang Rong, Shuqing Wang (2002). Multivariate predictive control applied in a industrial distillation column, process control science and technology(the corpus of the Thirteenth China Process Control Annual Conference), p360~364, South China University of Technology press, Guangzhou.